INVESTIGATION OF THE SUITABILITY OF THE BISCATECHOLBORATE ANION AS A REDUCTIVE QUENCHER FOR PHOTOEXCITED RUTHENIUM POLYPHYRIDYL COMPLEXES

by

ALPER YARASIK

Presented to the Faculty of the Graduate School of

The University of Texas at Arlington in Partial Fulfillment

of the Requirements

for the Degree of

MASTER OF SCIENCE IN CHEMISTRY

THE UNIVERSITY OF TEXAS AT ARLINGTON

August 2006

ACKNOWLEDGEMENTS

I would like to extend my thanks to Dr. MacDonnell for giving me the great opportunity to study in his laboratory. Dr. MacDonnell led and helped me to achieve my goals to be a good scientist and also encouraged me to take the next step on this field. He is a great leader who told us, his project team, how to work, study and focus on a particular subject. Besides, he spent his time by doing experiments with us. In addition, I have gained a great deal of experience by working with Dr. MacDonnell, by meeting and discussing about the project within a team. Finally, once again I would like to thank him for his understanding, patience, and sense of humor.

My thesis committee, Dr. Rasika Dias and Dr. Norma de Tacconi, provided me suggestions and directions along my project. I gratefully thank to them for their efforts.

Also, I would like to take this opportunity to express gratitude to all my colleagues and staff at Chemistry Department, UTA, for their generous help and support: Tamara Janatne, Kelly Wouters, Fiona Ongeri, Shelly Hampe, Rita Anderson and Ruth Handly.

I am grateful to my parents; Recai, Kiymet, and my sister Gulper Yarasik for their enormous encouragement and support. Finally, I want to express my deep appreciation to my lovely fiancée, Yeliz Ergune, for her enthusiasm, love and understanding.

April 15, 2006

ABSTRACT

INVESTIGATION OF THE SUITABILITY OF THE BISCATECHOLBORATE ANION AS A REDUCTIVE QUENCHER FOR PHOTOEXCITED RUTHENIUM POLYPHYRIDYL COMPLEXES

Publication No. _____

Alper Yarasik, M. S.

The University of Texas at Arlington, 2006

Supervising Professor: Frederick M. MacDonnell

Ruthenium polypyridyl complexes $[Ru(L\text{-}L)_3]^{2+}$, (L-L = 1,10 - phenanthroline or 2,2'-bipyridine) which covalently linked to electron donor or acceptor units are frequently used in artificial photosystems because of their high emission quantum yields, long excited-state lifetimes, favorable redox properties and excellent chemical stability. The ruthenium dimer **P,** $[(phen)_2Ru(tatpp)Ru(phen)_2][PF_6]_4$, undergoes multiple photo-reductions in the presence of electron donors such as triethylamine (TEA); however, large amount of donors (0.3 M) are required for efficient reductions. This research explores the use of a anionic donor such as $[B(cat)_2]^-$ with the hypothesis that ion-pairing will result in lower required concentration of the electron donor. Electrochemical data reveals that $[B(cat)_2]^-$ is oxidized irreversibly;

therefore, it can be used as a sacrificial donor. Stern-Volmer quenching of $[Ru(bpy)_3]^{2+}$ with $[B(cat)_2]^-$ and the photochemistry of complex $\mathbf{P^{4+}}$ with $[B(cat)_2]^{-1}$ conducted to examine its usefulness for this application.

Replacement of the bridging ligand of photoactive Ru complex P^{4+} (tatpp for 9,11,20,22-Tetraazatetrapyrido[3,2-*a: 2*', 3'-c:3'', 2''- l: 2''', 3'''-n]pentacene) with bdppz (for 1,19-dipyrido[3,2-*a*:29,39-*c*]phenazin-1,19-yldipyrido[3,2-*a*:29,39-*c*]-phenazine) results in interesting electronic and redox properties. The first and second reduction potentials of the resultant complex ($[(phen)_2Ru(dppz)$-$(dppz)Ru(phen)_2]^{4+}$, $\mathbf{1^{4+}}$) are reported by De Cola and coworkers[34]. The cyclic voltammetry data revealed two sequential one electron reductions and interestingly both first and second reduction potentials (BD/BD^- = -0.683 and BD^-/BD^{2-} = -0.873 vs NHE) are more negative than the ruthenium complex $\mathbf{P^{4+}}$ (P^{4+}/P^{3+} = -0.02 and P^{3+}/P^{2+} = -0.513 vs NHE)**.** Thus, the species are more reductive which could be used in another application such as photo-splitting water.

TABLE OF CONTENTS

ACKNOWLEDGEMENTS ii

ABSTRACT iii

LIST OF ILLUSTRATIONS viii

LIST OF TABLES x

Chapter

1. INTRODUCTION …….. 1

1.1 Ru Complexes as Photosensitizers..... 1

1.2 Electron Transfer Quenching 4

1.3 Quenching Rate and Mechanism 6

1.4 Sacrificial Reducing Agents …… 9

1.5 Scope of thesis dissertation ……..... 12

2. INVESTIGATION OF THE SUITABILITY OF THE BISCATECHOLBORATE ANION AS A REDUCTIVE QUENCHER FOR PHOTOEXCITED RUTHENIUM POLYPHYRIDAL COMPLEXES…… 13

2.1 Introduction……..... 13

2.2 Results and Discussion……. 19

2.2.1 Electrochemistry……. 19

2.2.2 Reductive Quenching of the Ruthenium Complex Excited State..... 21

2.2.3 Photochemical reduction of Ru complex, $\boldsymbol{P^{4+}}$ *with* $[B(cat)_2]^{-1}$ ……..... 28

2.3 Conclusion……. 34

2.4 Experimental Section …… 35

2.4.1 Materials ……...……... 35

2.4.2 Instrumentation …….. 35

2.4.3 Photochemical studies …… 36

2.4.4 Rate Studies …… 36

2.4.5 Quenching of $\boldsymbol{P^{4+}}$ *with TEA and* $[B(cat)_2]^-$ ……..…… 37

3. ELECTROCHEMICAL AND PHOTOCHEMICAL

REDUCTION OF $[(phen)_2Ru(dppz)\text{-}(dppz)Ru(phen)_2]^{4+}$ DIMER..... 38

3.1 Introduction……..... 38

3.2 Results and Discussion……... 41

3.2.1 Electrochemical Reduction and Protonation…...…….. 41

3.2.2 Chemical Reduction and Protonation of $\boldsymbol{1^{4+}}$…..…… 43

3.2.3 Photochemical Reduction of $\boldsymbol{1^{4+}}$ *with TEA* ..…….……...……. 46

3.3 Experimental Section ……..... 49

3.5.1 Photochemical Studies……... 49

3.5.2 Chemical reductions of $\boldsymbol{1^{4+}}$ *with* $Co(Cp)_2$…...…….…….. 49

APPENDIX

A. THE UV-VIS SPECTRUM OF P^{4+} IN THE PRESENCE OF $[B(cat)_2]^{-1}$ ….. 50

B. SYNTHESIS SCHEME OF $[B(cat)_2]^-$, $\mathbf{P^{4+}}$ AND $\mathbf{1^{4+}}$…….. 54

C. ^{1}H NMR OF "$\mathbf{P^{4+}}$", "$\mathbf{1^{4+}}$" AND $[B(cat)_2]^-$…….. 61

D. STERN VOLMER PLOT OF $[Ru(bpy)_3]^{2+}$ WITH TEA AND $[B(cat)_2]^{-1}$..... 65

REFERENCES.. ……... 70

BIOGRAPHICAL INFORMATION…… 74

LIST OF ILLUSTRATIONS

Figure Page

1.1 Electron Transfer in $[Ru(L\text{-}L)_3]^{2+}$ Complexes..... 3

1.2 Generalized sketch of Sentisizer quenching..... 4

1.3 Quenching of $[Ru(bpy)_3]^{2+}$ 8

1.4 Examples of most common sacrificial reducing agents 9

2.1 Modified Latimer-diagram of the redox potentials of. $[Ru(bpy)_3]^{2+}$ in its ground and photoexcited state. Potentials quoted versus NHE. [22] ……. 14

2.2 **a)** *Cyclic Voltammogram* of $[TMA][B(cat)_2]$ (30 μM) in MeCN containing 0.1 M nBu_4NPF_6 as supporting electrolyte. Scan rate = 100 mV/s. Ag/AgCl reference electrode **b)** DPV of $[TMA][B(cat)_2]$ (30 μM) in MeCN containing 0.1 M nBu_4NPF_6 as supporting electrolyte. Ag/AgCl reference electrode. Pulse amplitude = 0.02 V, step size = 0.004 V, pulse duration = 0.2 s …….. 20

2.3 Stern-Volmer Plot of 10 μM $[Ru(bpy)_3]^{2+}$ and $[B(cat)_2]^-$ in MeCN. Excitation at 451 nm …….. 22

2.4 Stern-Volmer Plot of 10 μM $[Ru(bpy)_3]^{2+}$ and $[B(cat)_2]^{-1}$ (●) no salt (■) 0.0025 M NH_4PF_6 (▲) 0.025 M NH_4PF_6 in MeCN…… 23

2.5 Stern-Volmer Plot of 10 μM $[Ru(bpy)_3]^{2+}$ and Triethylamine in (●) no salt (■) 0.0025 M NH_4PF_6 (▲) 0.025 M NH_4PF_6 in MeCN……... 25

2.6 The visible spectrum of $\mathbf{P^{4+}}$ (19 μM) in the presence of 50 mM of $[B(cat)_2]^-$ in degassed acetonitrile / 10% water during photoirradiation [100 W tungsten bulb (light source), 360 nm cutoff filter] ; a) 0 to 15 minutes b) 15 to 110 minutes…….... 30

2.7 The visible spectrum of $\mathbf{P}^{4+}$ (19 μM) in the presence of 50 mM of $[B(cat)_2]^{-1}]^-$ in degassed acetonitrile / 10 % 0.1 M NaOH during Photoirradiation [100 W tungsten bulb (light source), 360 nm cutoff filter]… 31

2.8 Reductive quenching of photoexcited complex $\mathbf{P}^{4+}$ in the presence of $[B(cat)_2]^-$ vs TEA as monitored by the appearance of $\mathbf{P}^{3+}$ (at 975 nm) Condition: (•) $\mathbf{P}^{4+}$ (19μM) and $[B(cat)_2]^-$ (50 mM) in degassed MeCN / 10 % water (+) $\mathbf{P}^{4+}$ (19μM) and TEA (50 mM) in degassed MeCN / 10 % water Irradiation: 100 W Tungsten bulb (360 nm cutoff) at 23°C for 45 minutes... 33

3.1 Reduction States of $\mathbf{1}^{4+}$ ……. 41

3.2 a) UV/Vis spectra of $\mathbf{1}^{4+}$ (——), $\mathbf{1}^{3+}$ (·····) and $\mathbf{1}^{2+}$(— · · —) in butyronitrile/ 0.3 M Bu_4NPF_6, recorded in an OTTLE cell b) UV/Vis spectra of $\mathbf{H_2 1}^{4+}$ chemical reduction with Zn in deaerated acidified acetonitrile[23]…….. 43

3.3 Absorption spectra of $\mathbf{1}^{4+}$, $\mathbf{1}^{3+}$ and $\mathbf{1}^{2+}$ in acetonitrile as generated in situ via stoichiometic reductions with $Co(Cp)_2$…… 46

3.4 Chemical reduction of $\mathbf{1}^{4+}$ using sodium borohydride in 10 % water/ MeCN …… 47

3.5 The visible spectrum of $\mathbf{1}^{4+}$ (19 μM) in the presence of 0.3 M TEA in degassed acetonitrile during photoirradiation[100 W tungsten bulb (light source), 360 nm cutoff filter] a)0-15 minutes b) 15-60 minutes…… 50

3.6 The visible spectrum of $\mathbf{1}^{4+}$ (19 μM) in the presence of 0.3 M TEOA in degassed water during photoirradiation [100 W tungsten bulb (light source), 360 nm cutoff filter]……... 51

LIST OF TABLES

Table Page

2.1 Quenching constants of $[Ru(bpy)]^{2+}$ in the presence of NH_4PF_6 25

2.2 Reduction Potential and Quenching Constant of Common Donors…… 27

3.1 First and second reduction potentials of $\mathbf{P}^{4+}$ and $\mathbf{1}^{4+}$ 39

CHAPTER 1

INTRODUCTION

1.1 Ru Complexes as photosensitizers

The photocleavage of water into hydrogen and oxygen has attracted considerable attention because of its potential to generate environmentally friendly H_2 fuel. The chemical energy per mole of hydrogen (approximately 142 MJ kg^{-1}) is at least three times larger than that of hydrocarbon fuels (approximately 47 MJ kg^{-1})[1]. Combustion of hydrogen produces only water which is clean and it does not result in harmful emissions into the environment. Therefore, much effort has been invested on using solar energy to decompose water into hydrogen.[2-4]

Ru(II) complexes has been investigated in the development of artificial systems for photochemical energy conversion. Especially, Ruthenium polypyridyl complexes of the type $[Ru(L\text{-}L)_3]^{2+}$, (L-L = 1,10 - phenanthroline or 2,2'- bipyridine) are promising chromophore for artificial photosystem because of their high emission quantum yields, long excited-state lifetimes, favorable redox properties and excellent chemical stability.[5] The photo excited state of interest is formed by metal to ligand charge transfer (MLCT) transition which occurs at 480 nm. In the excited state, the complex can formally be viewed as a transient charge separated complex, $[Ru^{3+}(L\text{-}L)_2(L\text{-}L^{-})]$ (or $[Ru(L\text{-}L)_3]^{2+*}$ in short) which can act as both an oxidizing and a reducing agent as shown in reaction 1 and 2.

$[Ru(L\text{-}L)_3]^{2+*} + e^- \longrightarrow [Ru(L\text{-}L)_3]^+$ Electron Acceptor (1)

$[Ru(L\text{-}L)_3]^{2+*} \longrightarrow [Ru(L\text{-}L)_3]^{3+} + e^-$ Electron Donor (2)

The $[Ru(bpy)_3]^{2+*}$ photo excited-state has a lifetime of 600 ns to 1200 ns depending on the solvent and temperature. The excited state can be quenched via electron transfer process. Electron transfer quenching can occur via reductive (Eq. 1) or oxidative (Eq. 2) pathways with suitable electron transfer groups. As shown in Figure 1.1, reductive quenching of $[Ru(L\text{-}L)_3]^{2+*}$ leads to $[Ru(L\text{-}L)_3]^+/ D^+$ which is produced by transferring an electron from the HOMO of the metal complex to the LUMO of the quencher. The charge separated state can be deactivated by back electron transfer from metal complex to the quencher.[6-8]

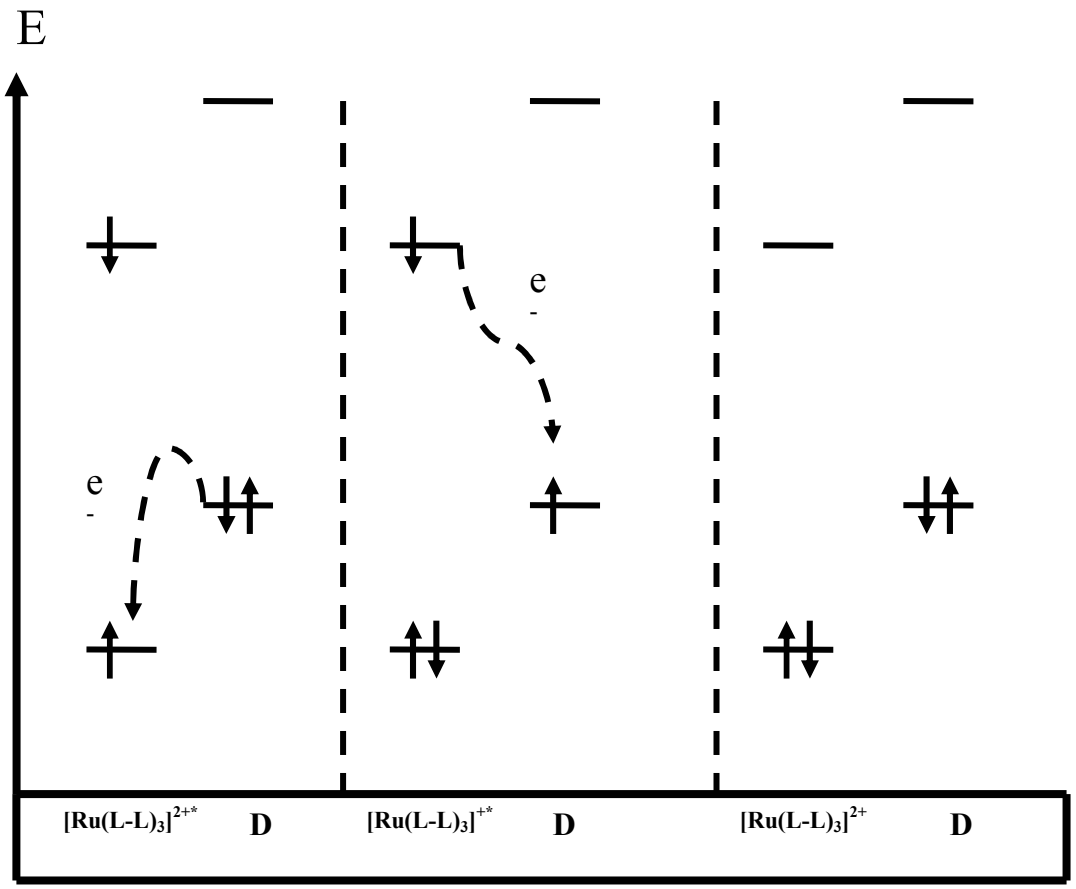

Figure 1.1 Electron Transfer in $[Ru(L\text{-}L)_3]^{2+}$ Complexes

1.2 Electron Transfer Quenching

The development of an effective sensitizer for electron transfer is fundamental to the chemical conversion of solar energy. The central importance is the improvement of the charge separation yield. In order to obtain high quantum yield of charge separation the use of sacrificial reductant and oxidants is essential. In reductive quenching, suitable sacrificial electron donors must be used to prevent the back electron transfer between primary photoproducts resulting in recover of the starting material.[9, 10] Reductive quenching yields the strongly reducing $[Ru(L\text{-}L)_3]^+$ species which can react readily with superior sensitizer such as MV^{2+}.

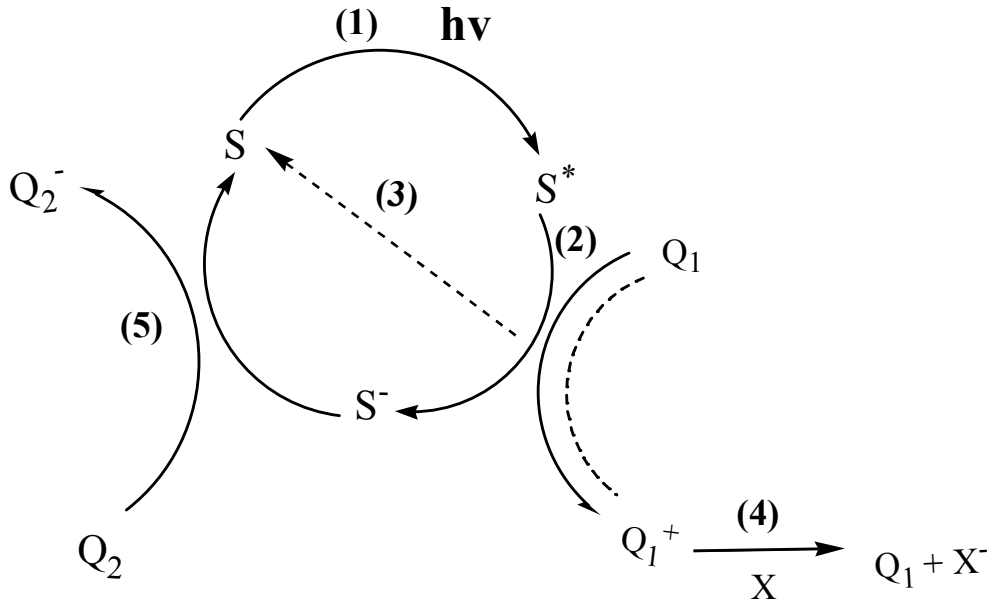

Figure 1.2 Generalized sketch of sensitizer quenching

As shown in figure 1.2 the photoexcitation of sensitizer (S) is followed by either oxidative or reductive quenching. The oxidized or reduced form may be recycled to regenerate the sensitizer (S) by process 3 or by process 5. Process 3 which is known as back electron transfer competes with product forming process 4 and the forward electron process 5. If process 3 dominates, no net chemical reaction is observed and the photo energy is thermalized.

Back electron transfer can be prevented by introducing columbic repulsive interaction between the sensitizer and quencher. The columbic repulsion keeps the species apart which minimizes the ability for back electron transfer. If the columbic interaction is the main driving force in process 3, in the presence of similarly charged species, the charge-separation quantum yield increases.[11-13]

1.3 Quenching Rate and Mechanism

The emission lifetime of an emitted excited state can be shortened (quenched) by addition of a chemical reagent that reacts with the excited state. These quenching reactions appear in triplet phosphorescent states because their excited lifetimes are sufficiently long for bimolecular reactions to occur. In the absence of any ground state bimolecular association between the complex and the quencher, the maximum rate is controlled by diffusion between two interacting molecules. Quenching rates can be obtained either measuring the excited-state lifetime in the presence of different concentrations of quencher or with the Stern-Volmer equation.

When light is shone on a solution of Ru polypyridyl complex, it may absorb the light and in the process get converted to one of its excited singlet states. If a state other than the lowest excited singlet state becomes populated, the molecule will rapidly relax to the lowest excited singlet state (M^*).

$$M + h\nu \underset{k_{-1}}{\overset{k_1}{\rightleftharpoons}} M^*$$

This excited state can emit a photon and in the process get converted back to the ground state. This is fluorescence and the fluorescence decay process is a first-order rate process with a rate constant denoted by k_f.

A second possibility is for the excited molecule to lose its energy in the form of heat rather than light. In this nonradiative process, the Ru polypyridyl complex either gets converted back to ground state (internal conversion) or to the lowest triplet state (intersystem crossing) and then the ground state. Both routes result in the disappearance

of the single excited-singlet state without the emission of light and can be lumped together in a first-order rate process with rate constant denoted by k_{nr}.

Quantum yield of fluorescence can be calculated by dividing the rate of fluorescence by sum of the rates of both fluorescence and nonradiative decay.

$$\Phi_0 = \frac{k_f}{k_f + k_{nr}}$$

If a quencher is present in the solution, the excited state molecules are depleted. The reaction rate constant (k_q) of quenching reaction assumed as a second order rate constant.

$$\Phi = \frac{k_f}{k_f + k_{nr} + k_q[Q]}$$

The relative quantum yield can be obtained by dividing Φ_o to Φ which yields the Stern-Volmer expression:

$$\Phi_o / \Phi = \frac{kq}{k_f + k_{nr}}[Q] + 1$$

The relative quantum yield in this expression can be replaced by the relative fluorescence intensity I_O/I which is easily measured. A plot of I_o/I versus [Q] should yield a straight line with a slope $k_q/(k_f + k_{nr})$. Since the $k_f + k_{nr}$ value are known as intrinsic lifetime of the excited state, k_q for the specific quencher can be determined.[14-19]

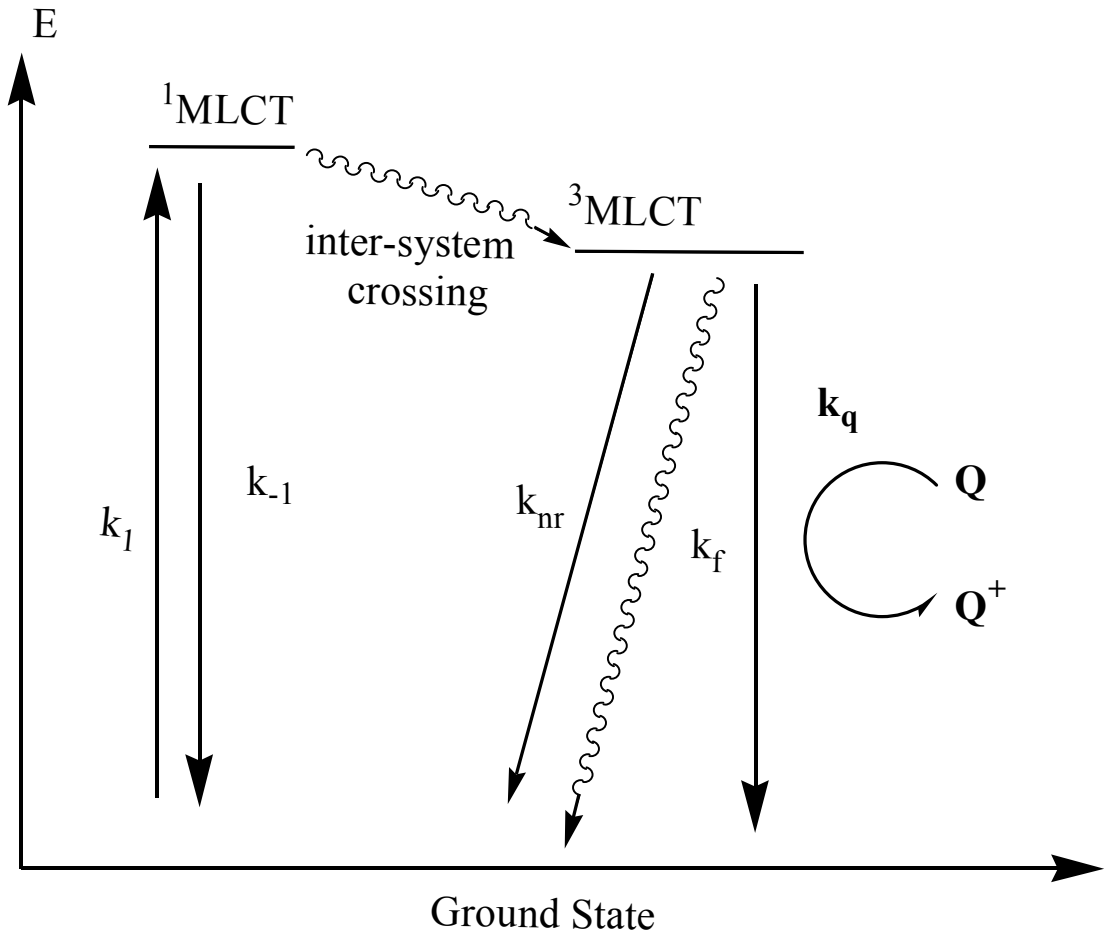

Figure 1.3 Quenching of $[Ru(bpy)_3]^{2+}$

1.4 Sacrificial Reducing Agents

In the presence of reductive quenchers Ru polypyridyl complexes undergo redox reactions. Triethylamine (TEA) and Ethylendiaminetetraacetic acid (EDTA) have been extensively used as electron donor in photochemical reactions. Their importance derives from the rapid and irreversible transformation of their one electron oxidized form (the radical localized on the amine moiety) into a carbon- localized reducing radical as the result of the loss of H^+ from the carbon atom α to the amino group.

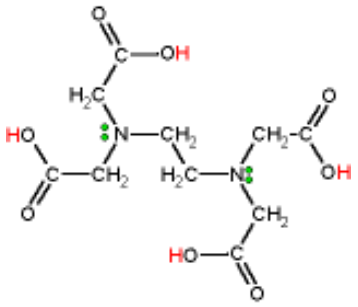

EDTA

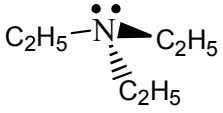

TEA

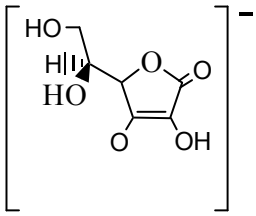

Ascorbate Ion

Figure 1.4 Examples of most common reducing agents

The generation of excited state with efficient reaction (reaction 1) is followed by the quenching of the Ru complex with an electron donor (2). The importance of the quenchers is derived by reaction 3 where the one electron oxidized form ($D_{ox}^{\cdot}$) is

transformed to the radical localized reduced form ($D_{red}^{\cdot}$) irreversibly. The reductive quenchers can be separated into three classes according to the nature of the radical localized reduced form ($D_{red}^{\cdot}$). Three classes of reductive quenchers are: sacrificial (TEA, EDTA, $C_2O_4^{2-}$), semi-sacrificial (thiols) and non-sacrificial (ascorbate ion) [20]. The one-electron oxidation of a sacrificial reducing agent forms oxidized species. However, with the semi-sacrificial reducing agents oxidation yields strongly reducing radicals in addition to the one-electron reducing agent. The oxidation products of non-sacrificial reducing agents do not transform instead they decay via molecular disproportionation[21].

$$[Ru(L\text{-}L)_3]^{2+} \xrightarrow{h\nu} [Ru(L\text{-}L)_3]^{2+*} \quad \textbf{(1)}$$

$$[Ru(L\text{-}L)_3]^{2+*} + D \longrightarrow [Ru(L\text{-}L)_3]^{+} + D_{ox}^{\cdot} \quad \textbf{(2)}$$

$$D_{ox}^{\cdot} \longrightarrow D_{red}^{\cdot} \quad \textbf{(3)}$$

Since the realization that the metal-to-ligand charge-transfer state (MLCT) of $[Ru(bpy)_3]^{2+}$ (bpy = 2,2'-bipyridine) could undergo excited-state electron transfer, a series of studies have been undertaken to utilize this fact in solar energy conversion schemes.[22] One of the ultimate goals is to produce fuels that involve the transfer of multiple electrons to a substrate. Unfortunately, $[Ru(bpy)_3]^{2+}$ can only transfer a single electron to a substrate without the incorporation of a secondary material to function as an electron collector. Consequently, much effort has focused on the development of

polymetallic systems which incorporate multiple $[Ru(bpy)_3]^{2+}$ moieties in the same molecule[23, 24].

The Ruthenium complex $\mathbf{P^{4+}}$, $[(phen)_2Ru(tatpp)Ru(phen)_2][PF_6]_4$, (where phen is 1,10-phenanthroline and tatpp is 9,11,20,22-tetraaza tetrapyrido[3,2-a:2'3'-c:3",2"-l:2"',3"']-pentacene) is an example of a bi-metallic species which incorporates two light absorbing moieties with the tatpp bridge. The photo-reduction of complex **P** in the presence of triethylamine (TEA) can generate species capable of storing up to two electrons. This is significant because the hydrogen generation process is also two electron reduction.[25, 26]

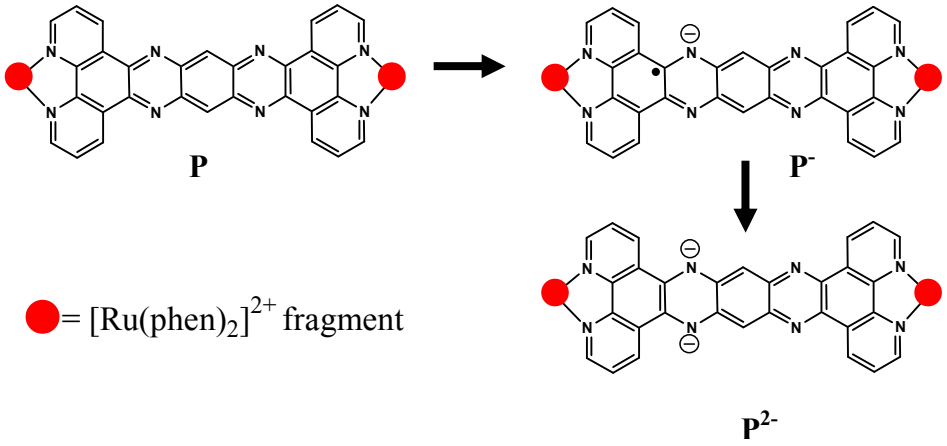

1.5 Scope of Thesis Dissertation

Previous studies of complex $\mathbf{P}^{4+}$ with TEA as a sacrificial reducing agent show that the photo-reduction of complex $\mathbf{P}^{4+}$ is two-electron reduction. In order to have an efficient photochemical process, the concentration of the Ru complex and sacrificial reducing agent must be optimized to prevent thermal reductions. An ideal 'sacrificial' reducing agent would function well at low concentrations, and be reversibly oxidized. In the second chapter, the photochemistry of a novel sacrificial reducing agent, biscatecholborate ($[B(cat)_2]^{-1}$), with ruthenium complex, $\mathbf{P}^{4+}$, will be discussed. The reaction rate of $\mathbf{P}^{4+}$ with $[B(cat)_2]^-$ and TEA is compared by using Stern-Volmer quenching plots. In the third chapter, the bridge between the photoactive Ruthenium (II) centers is replaced with bdppz (1,19-dipyrido[3,2-*a*:29,39-*c*]phenazin-1,19-yldipyrido[3,2-*a*:29,39-*c*]phenazine) bridges in order to increase the reduction potential. In addition, the spectroelectrochemistry and photochemistry of the compound is studied with UV-Vis Absorption Spectroscopy.

CHAPTER 2

INVESTIGATION OF THE SUITABILITY OF THE BISCATECHOLBORATE ANION AS A REDUCTIVE QUENCHER FOR PHOTOEXCITED RUTHENIUM POLYPHYRIDYL COMPLEXES

2.1 Introduction

Ruthenium (II) polypyridyl complexes, such as $[Ru(bpy)_3]^{2+}$, are attractive sensitizers for driving redox reactions because of their excellent chemical stability, reversible redox properties and favorable photophysical properties.[27] A Latimer-type diagram for the photoexcited complex, shown in Figure 2.1, was constructed by Meyers and coworkers and shows the redox potentials for the various transformations of $[Ru(bpy)_3]^{2+}$ in the ground and photoexcited state. [28] Changes from bpy to a number of other diimine and triimine type ligands can be used to tune these redox potentials in either direction.[28]

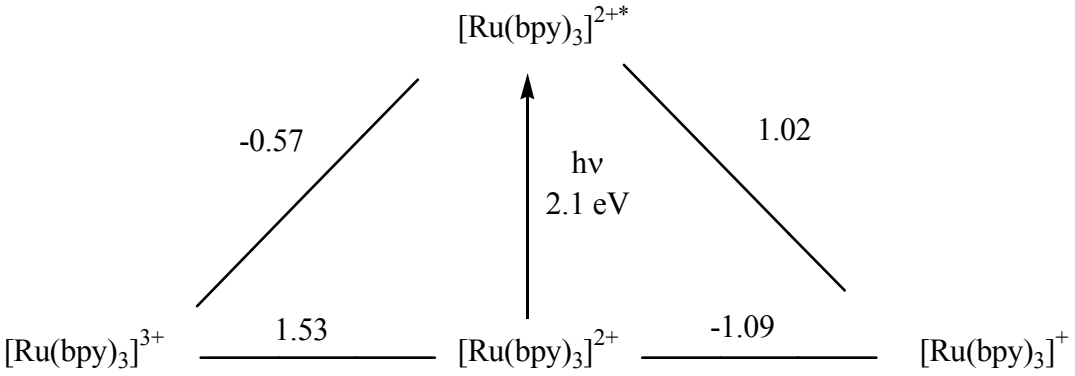

Figure 2.1 Modified Latimer-diagram of the redox potentials of $[Ru(bpy)_3]^{2+}$ in its ground and photoexcited state. Potentials quoted versus NHE. [28]

As can be seen, the photoexcited complex, denoted $[Ru(bpy)_3]^{2+*}$, is 2.1 eV higher in energy than the ground state and can act as either a potent oxidant (E_{ox} $Ru^{2+*/3+}$ = - 0.57 V) or reductant (E_{red} $Ru^{2+*/+}$ = 1.02 V). As shown in reactions 1 -3, reaction of the photoexcited complex with a number of donor or acceptor molecules results in the formation of stable reduced and oxidized ruthenium complexes, which are themselves potential reducing ($E^{2+/1+}$ = 1.09 V) and oxidizing ($E_{red}^{3+/2+}$ = 1.53 V) agents. Unfortunately, the back reactions (4 and 5) are often facile and lead to low quantum yields for charge separation.

$$[Ru(bpy)_3]^{2+} + h\nu \rightarrow [Ru(bpy)_3]^{2+*} \quad (1)$$

$$[Ru(bpy)_3]^{2+*} + D \rightarrow [Ru(bpy)_3]^{+} + D^{+} \quad (2)$$

$$[Ru(bpy)_3]^{2+*} + A \rightarrow [Ru(bpy)_3]^{3+} + A^{-} \quad (3)$$

$$[Ru(bpy)_3]^{+} + D^{+} \rightarrow [Ru(bpy)_3]^{2+} + D \quad (4)$$

$$[Ru(bpy)_3]^{3+} + A^{-} \rightarrow [Ru(bpy)_3]^{2+} + A \quad (5)$$

Nonetheless, it is possible (though challenging) to drive thermodynamically unfavorable redox reactions by utilizing these photocatalysts and light as the free energy source. One long sought goal of this research is to utilize such photocatalysts to capture and store solar energy in the form of high energy molecules (fuels), such as H_2. Perhaps the most desirable of all such energy conversion schemes would be the use of such photocatalysts to break water into H_2 and O_2 (the water-splitting reaction), shown in reaction 6.

$$2\ H_2O \xrightarrow{h\nu,\ Ru\ cat} 2\ H_2 + O_2 \qquad (6)$$

Such a scheme would allow us to utilize water as a fuel source, generate H_2 as the storable fuel and release O_2 directly into the environment. Recombination of the two gases whether in a fuel cell to generate electricity or by combustion to generate heat, produces only water as product and is thus both environmentally friendly and catalytic in water.

Currently, no viable water-splitting photocatalytic processes are known and a number of technical challenges remain to be conquered. One particular problem that this lab has focused on is overcoming the stoichiometry mismatch between metal-based photocatalysts, which typically are limited to one electron processes, and the multi-electron requirements of the water-splitting reaction. In the ruthenium polypyridine family, very few complexes are able to form a stable, doubly-reduced complex upon irradiation. If such doubly-reduced complexes could readily be formed, then it may be possible to drive the energetically easier two electron hydrogen-evolving reaction

(HER) (reaction 7) as opposed to the energetically difficult one electron reduction of H^+ to $H^\cdot$ followed by coupling the $H^\cdot$ atoms (reactions 8 and 9). Clearly, distinct energetic advantages can be realized by developing catalysts capable of driving multi-electron reactions.

$$2\ H^+(aq) + 2\ e^- \rightarrow H_2(g) \quad E = -0.41\ V\ (at\ pH\ 7) \qquad (7)$$

$$H^+(aq) + e^- \rightarrow H^\cdot(aq) \quad E = -2.69\ V \qquad (8)$$

$$2\ H^\cdot(aq) \rightarrow H_2(g) \qquad (9)$$

The trimetallic complex, $[\{(bpy)_2Ru(2,3\text{-bis(pyridyl)-benzoquinoxaline})\}_2IrCl_2]^{4+}$, was the first complex shown to photochemically store two electrons upon reductive quenching with a sacrificial donor (dimethylaniline).[23] Subsequently, we showed that the photoactive Ru(II) dimers, $[(phen)_2Ru(tatpp)Ru(phen)_2]^{4+}$ ($\mathbf{P}^{4+}$) and $[(phen)_2Ru(tatpq)Ru(phen)_2]^{4+}$ ($\mathbf{Q}^{4+}$) could stored up to two or four electrons, respectively, upon visible irradiation in the presence of sacrificial donors.[25]

While our success in storing multiple reducing equivalents on $\mathbf{P}^{4+}$ and $\mathbf{Q}^{4+}$ we have been focused on the HER, ultimate success will also require driving the other half-reaction – the oxygen evolving reaction (OER, see reaction 10).

$$2\ H_2O(l) \rightarrow O_2(g) + 4\ H^+(aq) + 4\ e^- \quad E = 0.82\ V\ (pH\ 7) \qquad (10)$$

Currently, organic amines, such as triethylamine (TEA), triethanolamine (TEOA) and dimethylaniline (DMA), are used as sacrificial donors to generate the reduced metal complex. The oxidized products are radical cations (D^+) which rapidly decompose and thereby prevent a charge recombination reaction between the reduced metal complex and the oxidized amine. While this provides a convenient method of photochemically generating reduced ruthenium complexes, e.g., $[Ru(bpy)_3]^+$, it is not practical to use organic amines stoichiometrically as donor molecules in any real solar energy conversion scheme. Ideally, the sacrificial donor would be water and O_2 would be the byproduct. Unfortunately, neither the photoexcited complex $[Ru(bpy)_3]^{2+*}$ nor $[Ru(bpy)_3]^{3+}$ are directly capable of water oxidation even though they have the necessary oxidizing potential (at pH 7 or higher). Success therefore will likely require co-catalysts and donor molecules capable of relaying these redox equivalents between the Ru photocatalyst and the OER co-catalyst.

This chapter explores a potential new electron donor complex, biscatecholborate or $[B(cat)_2]^-$, as a redox shuttle for oxidizing equivalents with several desirable characteristics. First of all, the complex is anionic and expected to form ion-pair with the cationic ruthenium photocatalyst and therefore should show high quantum yields of charge separation. Secondly, the oxidized complex, $[B(cat)_2]^0$, is neutral and therefore it should easily dissociate from the ruthenium complex and be replaced by another anion. This favorable dissociation kinetics should also improve quantum yield by inhibiting charge recombination back reactions (e.g., reaction 4). Thirdly, the oxidation is likely to be reversible as the catechol/semiquinone couple involved is readily reversible. And

fourth, the oxidation potential of the $[B(cat)_2]^{-1/0}$ couple is expected to be comparable with those for organic amines. These values are close to the oxidizing potential of $[Ru(bpy)_3]^{2+*}$. By minimizing the free energy lost as heat during the reductive quenching of $[Ru(bpy)_3]^{2+*}$ we maximize the free energy that can be used to drive subsequent reactions. In this chapter, we report on the electrochemical properties of $[N(CH_3)_4][B(O_2C_6H_4)_2]$ and its use as a donor in photochemical reactions with both $[Ru(bpy)_3]^{2+}$ and $[(phen)_2Ru(tatpp)Ru(phen)_2]^{4+}$ ($\mathbf{P}^{4+}$).

2.2 Results and Discussion

2.2.1 Electrochemistry

The redox properties of $[B(cat)_2]^{-1}$ were examined by cyclic voltammetry (CV) and differential pulse voltammetry (DPV) and the results are shown in Figures 2.2. The CV of the $[B(cat)_2]^-$ anion shows two irreversible redox processes at approximately +0.90 and +1.25 V (E_{peak}) versus Ag/AgCl. From the DPV data, we obtained better estimates of the formal potentials at +0.80 V and +1.14 V versus Ag/AgCl and will use these values in any future discussion of the redox potentials for $[B(cat)_2]^-$. The redox processes are assigned to the $[B(cat)_2]^{0/-1}$ and $[B(cat)_2]^{+1/0}$ couples, the first of which is most likely involving a catechol centered oxidation to form the semiquinone species shown in reaction 11.

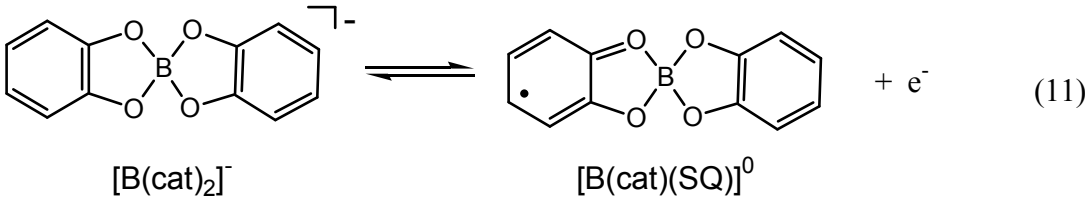

(11)

The second oxidation process either completes the oxidation of the semiquinone (SQ) to the quinone (Q) to give $[B(cat)(Q)]^+$ or is the oxidation of the second catechol to SQ to yield, $[B(SQ)_2]^+$. The fact that neither process is reversible shows that the $[B(cat)(SQ)]^0$ complex is very reactive and is lost either via ligand dissociation or by radical chemistry of the SQ species. CV's in which the scan was reversed after the first oxidation process but before the second oxidation were similarly irreversible.

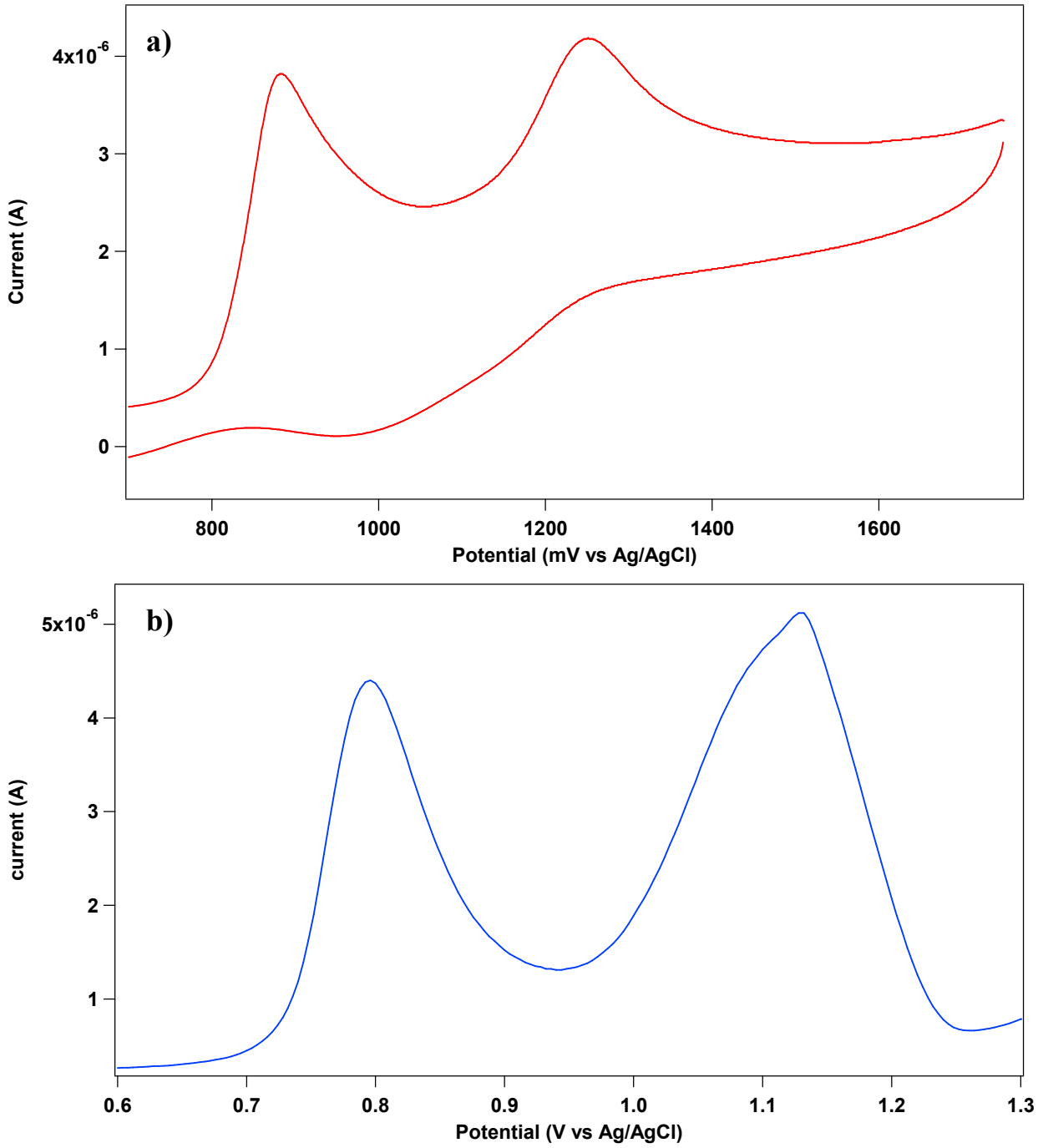

Figure 2.2 a) *Cyclic Voltammogram* of [TMA][B(cat)$_2$] (30 μM) in MeCN containing 0.1 M nBu_4NPF_6 as supporting electrolyte. Scan rate = 100 mV/s. Ag/AgCl reference electrode **b)** DPV of [TMA][B(cat)$_2$] (30 μM) in MeCN containing 0.1 M nBu_4NPF_6 as supporting electrolyte. Ag/AgCl reference electrode. Pulse amplitude = 0.02 V, step size = 0.004 V, pulse duration = 0.2 s

The cyclic voltamogram scan of $[B(cat)_2]^{-1}$ results in two irreversible one electron reduction waves ($E_{1/2}$ = 0.99 V and $E_{1/2}$ = 1.34 V vs NHE) while the reduction potential of $TEA^{0/+1}$ is $E_{1/2}$= 1.00 V vs NHE.[29] Therefore, the oxidized species of $[B(cat)_2]^{-1/0}$ has more reducing power than the oxidized species of $TEA^{0/-1}$.

2.2.2 Reductive Quenching of the Ruthenium Complex Excited State

Quenching rate constants are readily determined using the Stern-Volmer relationship given in equation 12.[18] In this analysis, the decrease (quenching) of

$$I_0/I = 1 + (k_q/ \tau_0) [Q] \qquad (12)$$

fluorescence intensity for the $[Ru(bpy)_3]^{2+*}$ luminophore is taken as a sign of electron transfer from the donor molecule/complex to the $[Ru(bpy)_3]^{2+*}$ complex as shown in reaction 13.

$$[Ru(bpy)_3]^{2+*} + D \rightarrow [Ru(bpy)_3]^{+} + D^{+} \qquad (13)$$

A typical quenching experiment involves the measurement of emission intensity of the excited state in the absence (I_0) and presence (I) of differing concentrations of the donor. Since the $k_f + k_{nr}$ value is known from intrinsic lifetime (τ_0) of the excited state, k_q for the specific quencher can be determined. The intrinsic lifetime (τ_o) for $[Ru(bpy)_3]^{2+*}$ is 0.67 μs.[22]

In order to test our technique, quenching rate constant (k_q) for TEOA with $[Ru(bpy)_3]^{2+}$ was evaluated and compared to the reported value of 1.7 x 10^5 $M^{-1}s^{-1}$ as reported by Hoffman and coworkers.[31] The Stern-Volmer plot (Appendix D) for this experiment shows the typical linear relationship of luminescent quenching with

increasing donor concentration. From the slope of this line and the Stern-Volmer relationship (equation 12), we obtained a k_q of 1.7 x 10^5 $M^{-1}s^{-1}$ which matches exactly with the value reported in the literature.

Addition of $[B(cat)_2]^-$ to an acetonitrile solution of $[Ru(bpy)_3]^{2+}$ results in also luminescence quenching. As shown in Figure 2.3, the Stern-Volmer plot of this with $[Ru(bpy)_3]^{2+}$ is linear and yields a k_q = 3.4 x 10^6 $M^{-1}s^{-1}$.

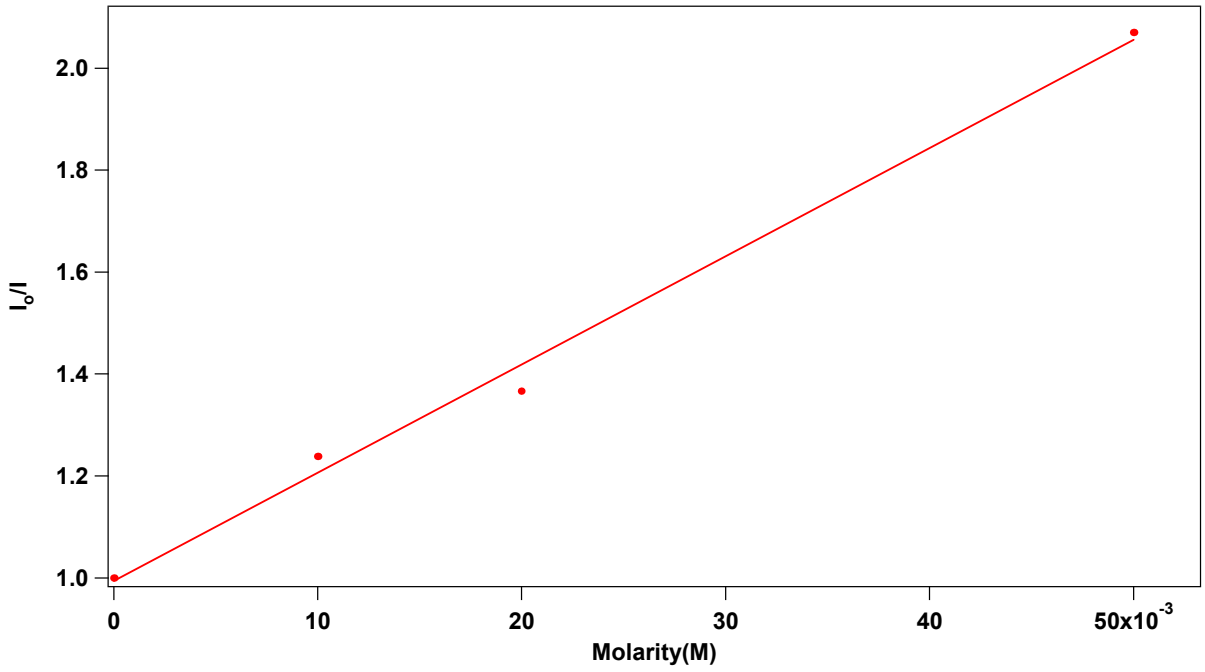

Figure 2.3 Stern-Volmer Plot of 10 μM $[Ru(bpy)_3]^{2+}$ and $[B(cat)_2]^-$ in MeCN. Excitation at 451 nm

It is assumed that ion-pairing between $[Ru(bpy)_3]^{2+}$ and $[B(cat)_2]^{-1}$ is an important factor in the efficiency of quenching with this donor. In order to test this

hypothesis, the ionic strength of the solution was raised by addition of an inert salt, NH_4PF_6. If ion-pairing is an important effect, then we expect a decrease in k_q for $[B(cat)_2]^{-1}$ as the ionic strength is raised as ion-pairing is effectively screened at higher ionic strength. Figure 2.4 shows the Stern-Volmer quenching plots of $[Ru(bpy)_3]^{2+}$ and $[B(cat)_2]^{-1}$ without andc with 0.0025 M and 0.025 M of NH_4PF_6. As can be seen the slopes decrease with increasing salt from a k_q of $3.41x10^6$ M^{-1} s^{-1} to 2.76×10^6 M^{-1} s^{-1} and 1.21×10^6 M^{-1} s^{-1} for 0.0025 M and 0.025 M $[NH_4PF_6]$, respectively. This represents a 65 % drop in quenching rate over this salt concentration and shows that the PF_6^- anion can effectively compete with $[B(cat)_2]^{-1}$ via ion-pairing.

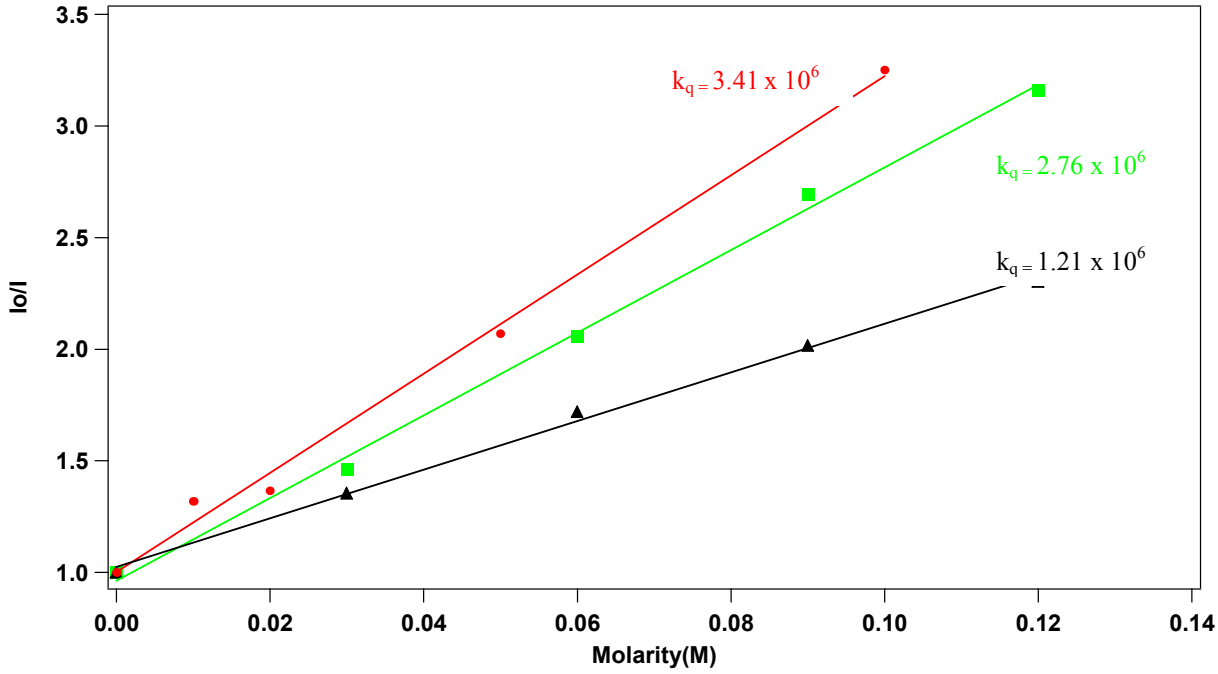

Figure 2.4 Stern-Volmer Plot of 10 µM $[Ru(bpy)_3]^{2+}$ and $[B(cat)_2]^{-1}$ (●) no salt (■) 0.0025 M NH_4PF_6 (▲) 0.025 M NH_4PF_6 in MeCN

TEA is a neutral compound and thus should not ion-pair with $[Ru(bpy)_3]^{2+}$. In order to show that increasing the ionic strength has little effect on other quenching mechanisms, e.g. solvent caged pairs, we examined the k_q of TEA as a function of ionic strength which can demonstrate that other types of quenching are unaffected by triethylamine which is another commonly used reductive quencher. Figure 2.5 shows the Stern-Volmer quenching of $[Ru(bpy)_3]^{2+}$ with TEA in MeCN without and with 0.0025 M and 0.025 M of NH_4PF_6, respectively. As can be seen, the slope is only slightly perturbed by addition of the salt, ranging from 1.3 $x10^6$ M^{-1} s^{-1} for no salt to 1.08 x 10^6 M^{-1} s^{-1} with 0.025 M added salt. As opposed to before when a 65% decrease in rate was observed, here the drop from no salt to 0.025 M salt is only 17%. The quenching rate constants for $[B(cat)_2]^{-1}$ and TEA is reported in Table 1.

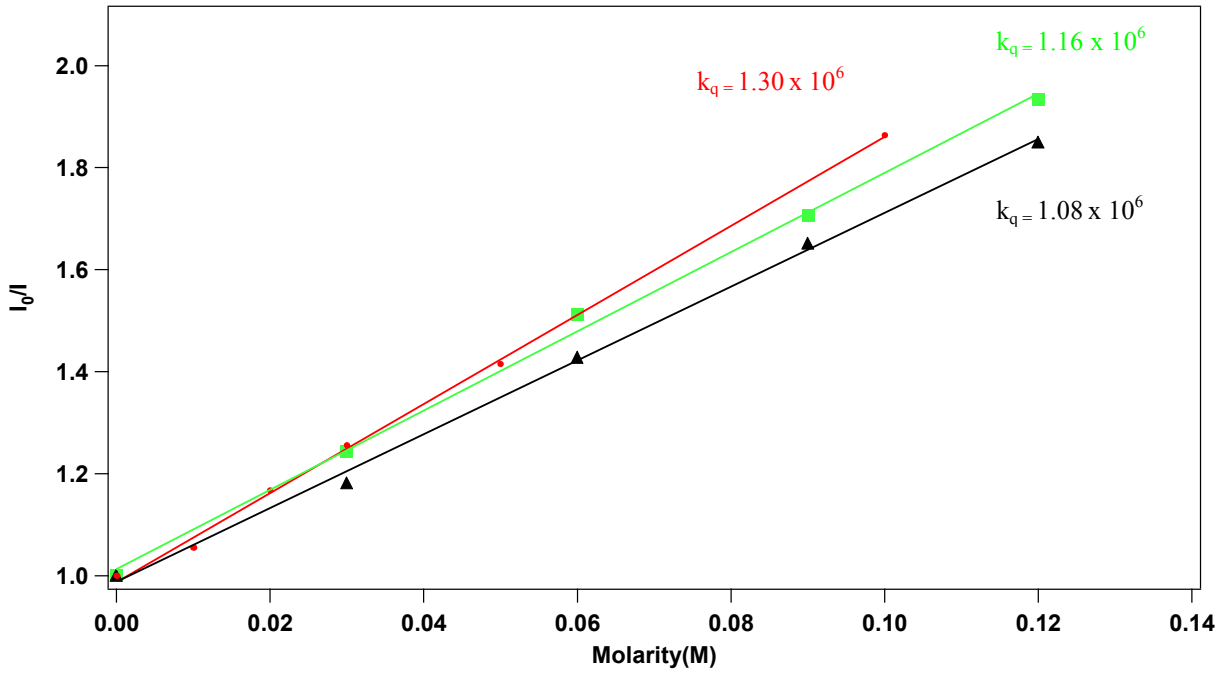

Figure 2.5 Stern-Volmer Plot of 10 µM $[Ru(bpy)_3]^{2+}$ and Triethylamine in (●) no salt (■) 0.0025 M NH_4PF_6 (▲) 0.025 M NH_4PF_6 in MeCN

Table 2.1 Quenching constants of $[Ru(bpy)]^{2+}$ in the presence of NH_4PF_6

Quencher / Concentration of salt	$[B(cat)_2]^{-1}$	TEA
No salt	$3.41 \times 10^6\ M^{-1}\ s^{-1}$	$1.30 \times 10^6\ M^{-1}\ s^{-1}$
0.0025 M NH_4PF_6	$2.76 \times 10^6\ M^{-1}\ s^{-1}$	$1.16 \times 10^6\ M^{-1}\ s^{-1}$
0.025 M NH_4PF_6	$1.20 \times 10^6\ M^{-1}\ s^{-1}$	$1.08 \times 10^6\ M^{-1}\ s^{-1}$

The effect of ion pairing on the quenching rate is seen more clearly when the ionic strength is modulated. The quenching rate of $[Ru(bpy)_3]^{2+}$ with $[B(cat)_2]^{-1}$ decreases approximately 65% in the presence of a competing ions, NH_4^+ and PF_6^-. We note that not all of this decrease can be attributed to ion-pairing effects as 17 % drop seen for TEA quenching. At higher ionic strength, other factors are at work, but clearly the majority of the effect is due to ion pairing.

The quenching rate constants for $[B(cat)_2]^{-1}$ and TEA with $[Ru(bpy)_3]^{2+}$ were also examined in the 10% water/MeCN mixture, as these conditions are required for reactivity with another ruthenium complex, **P**. The Stern-Volmer analyses of $[Ru(bpy)_3]^{2+}$ with $[B(cat)_2]^{-1}$ and TEA in 10% water/MeCN mixture give k_q's of 3.08 x 10^6 M^{-1} s^{-1} and 8.0 x 10^5 $M^{-1}s^{-1}$ respectively. At lower concentrations less than 5 μM, the Stern-Volmer plot with $[B(cat)_2]^{-1}$ is nearly horizontal presumably because the quenching is diffusion controlled.(Appendix E) At concentrations greater than 5 μM $[B(cat)_2]^{-1}$, the typical linear Stern-Volmer quenching relationship is seen with k_q calculated as 3.08 x 10^6 $M^{-1}s^{-1}$ which is almost 4 fold greater than TEA (8.0 x 10^5 $M^{-1}s^{-1}$).

The quenching and electrochemical data for TEA, TEOA and $[B(cat)_2]^{-1}$ are collected in Table 2.2. As can be seen, the reduction potential of the $[B(cat)_2]^{0/-1}$ couple is comparable with the organic amines commonly used as sacrificial reductants. The data presented in this table is referenced to NHE to permit easy comparison to the potentials for important water-splitting reactions, namely the HER and OER.

Table 2.2 Reduction Potential and Quenching Constants of Common Donors

Donors	**Couple**	**E_{red} (vs NHE)**	**k_q $(M^{-1}s^{-1})^b$**	**Solvent**	**Ref.**
$[B(cat)_2]^-$	0/-1	+0.99 [a]	3.4×10^6	MeCN	
			3.1×10^6	MeCN/10%H_2O	
DMA	+/0	+1.05 [a]	7.1×10^7	MeCN	31
TEA	+/0	+1.00 [a]	1.3×10^6	MeCN	
			8.0×10^5	MeCN/10%H_2O	
TEOA	+/0	+1.14 [a]	1.7×10^5	DMF	31, 32

[a] irreversible electrochemistry. [b] calculated using an instrinsic lifetime (τ) for $[Ru(bpy)_3]^{2+}$* of 0.67 μs.

The reduction potential of $[B(cat)_2]^{-1}$ is considerably larger than other common anionic donors, such as ascorbate ion and I^- (0.39 V and 0.62 respectively)[33], and thus potentially could 'store' more energy in the form of oxidizing potential (of the $[B(cat)_2]^0$ complex) if it could be made reversible. We note that the reduction potential of photoexcited $[Ru(bpy)_3]^{2+*/+1}$ is +1.02V thus when combined with the oxidation of $[B(cat)_2]^-$ as shown in reactions 14-16, the quenching process is nearly thermoneutral, meaning that little energy is wasted as heat.

$$[Ru(bpy)_3]^{2+*} + e^- \rightarrow [Ru(bpy)_3]^+ \qquad E = +1.02\ V \qquad (14)$$

$$[B(cat)_2]^- \rightarrow [B(cat)(SQ)]^0 + e- \qquad -0.99\ V \qquad (15)$$

$$[Ru(bpy)_3]^{2+*} + [B(cat)_2]^{-1} \rightarrow [B(cat)SQ] + [Ru(bpy)_3]^+ \quad +0.03\ V \qquad (16)$$

A similar analysis of reductive quenching of $[Ru(bpy)_3]^{2+*}$ with TEA yields a potential of +0.02 V, When these values are converted to free energy changes (n = 1 for both reactions), we observe that 1.93 kJ/mol of free energy are lost as heat in the TEA quenching

reaction compared to only 2.89 kJ/mol for the $[B(cat)_2]^-$ reaction. Both are near ideal but unfortunately not reversible.

2.2.3 Photochemical reduction of Ru complex, $\mathbf{P}^{4+}$, with $[B(cat)_2]^{-1}$

Our initial goal was to use $[B(cat)_2]^-$ as a reversible, high-oxidation potential donor to shuttle oxidizing equivalents (holes) from the photocatalyst $\mathbf{P}^{4+}$ to a co-catalyst. The irreversibility of the redox processes examined electrochemically shows that $[B(cat)_2]^-$ instead acts as a sacrificial donor that is consumed upon oxidation. We decided to examine the photoreduction of $\mathbf{P}^{4+}$ with $[B(cat)_2]^-$ to see if it indeed acts as a sacrificial donor and to evaluate the quantity needed for photoreduction. Both TEOA and TEA must be used in large excess (0.2 to 0.3 M) to successfully quench the photoexcited state in $\mathbf{P}^{4+}$ (~20 μM) and it is hoped that the ion-pairing interaction between $[B(cat)_2]^-$ and $\mathbf{P}^{4+}$ would lessen the requirements for such an excess of the sacrificial donor. Unfortunately, a mixture of $\mathbf{P}^{4+}$ and $[B(cat)_2]^{-1}$ in MeCN results in precipitation. However, precipitation can be prevented by adding water to the system and good solubility is obtained in 10% water:90% MeCN mixtures.

As shown in Figure 2.8, irradiation of a water/MeCN solution of $\mathbf{P}^{4+}$ (18.7 μM) and 50.0 mM of $[B(cat)_2]^-$ results in photoreduction. The appearance of a pair of bands at 860 and 970 nm is indicative of the formation of the singly reduced $\mathbf{P}^{3+}$ (Figure 2.8 a). With continued illumination, these long wavelength peaks begin to diminish and a new band at 635 nm is formed (Figure 2.8 b) which is suggestive of the doubly reduced complex $\mathbf{P}^{2+}$ with some protonation. The two reductive processes are completely reversible, and all of the redox

intermediates were seen to reappear and disappear in order until $\mathbf{P}^{4+}$ was completely regenerated. As the pH is known to strongly affect the photochemistry of $\mathbf{P}^{4+}$, the pH of this solution was controlled by a glass electrode.

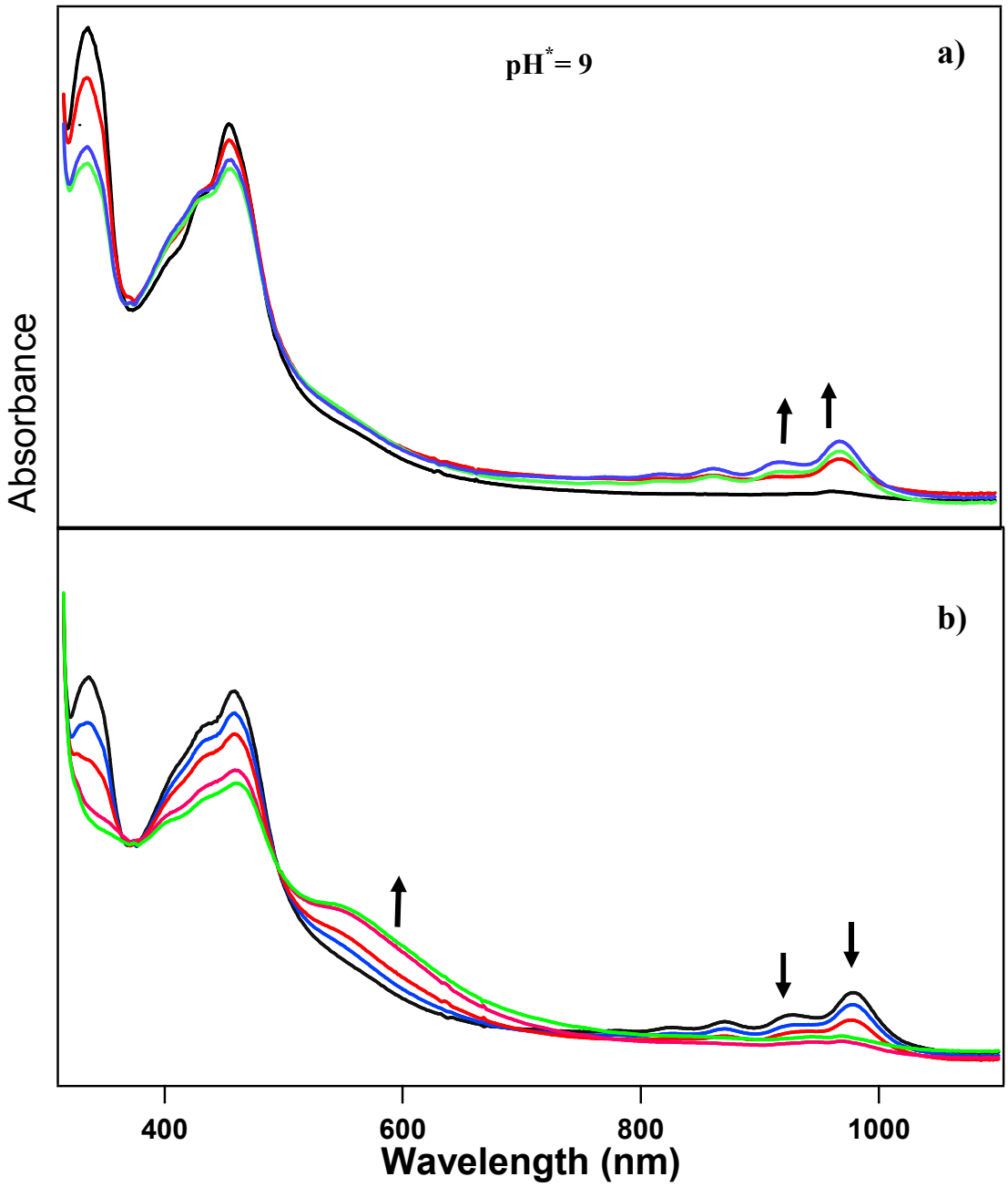

Figure 2.6 The visible spectrum of **P** (18.7 μM) in the presence of 50 mM of $[B(cat)_2]^-$ in degassed acetonitrile / 10% water during photoirradiation [100 W tungsten bulb (light source), 360 nm cutoff filter] ; a) 0 to 15 minutes b) 15 to 110 minutes

The pH was adjusted by addition of either HCl or NaOH and the photochemistry examined. At lower pH, no photochemistry is observed. At higher pH, the photochemistry is facilitated and the intensity of the bands corresponding to $\mathbf{P}^{3+}$ is higher under more basic conditions. In any case, the concentration of $[B(cat)_2]^-$ in these experiments (50 mM) is considerable less than the 250 to 350 mM concentrations of TEA or TEOA needed to affect a photoreduction of $\mathbf{P}^{4+}$ in a comparable time, suggesting that ion-pairing is one method by which the concentration of the sacrificial donor can be lessened.

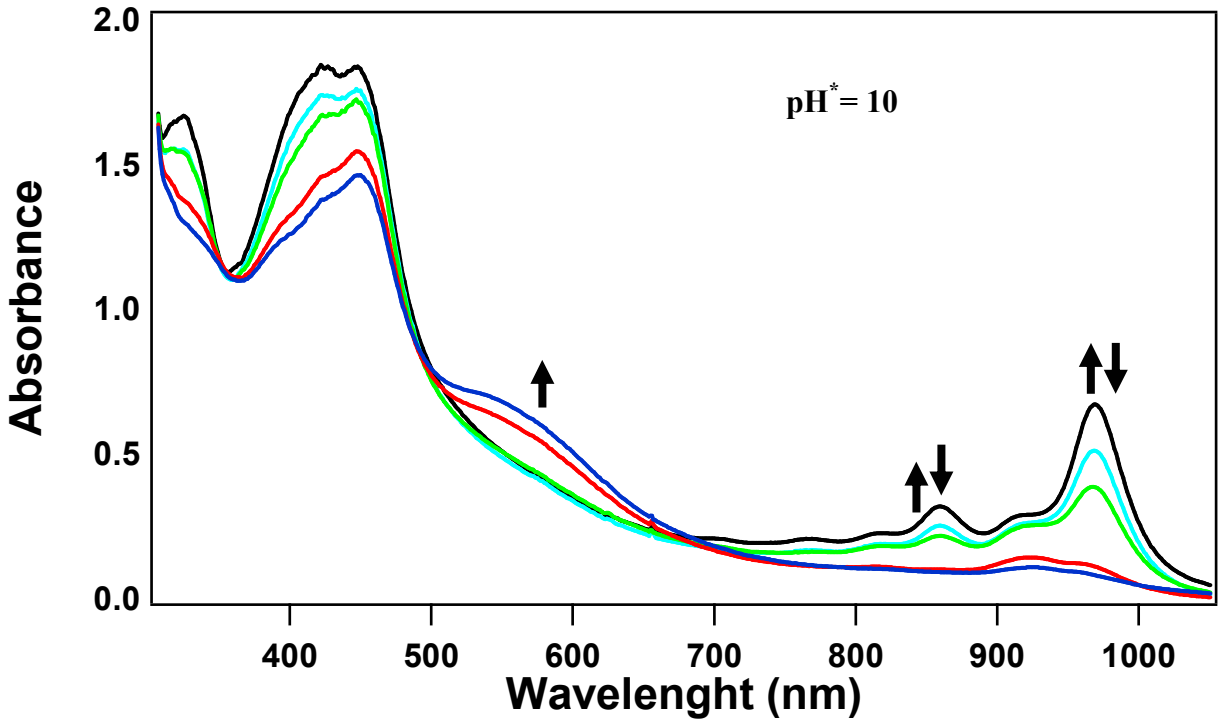

Figure 2.7 The visible spectrum of **P** (18.7 μM) in the presence of 50 mM of $[B(cat)_2]^-$ in degassed acetonitrile / 10 % 0.1 M NaOH during photoirradiation [100 W tungsten bulb (light source), 360 nm cutoff filter]

In addition to the Stern-Volmer analysis, the effect of the ion pairing in the reductive quenching of **P** can be examined by observing the effect on the rate of $\mathbf{P}^{3+}$ formation**.** As shown in Figure 2.8, the rate of photoreduction as measured by the increase in intensity of the 975 nm peak ($\mathbf{P}^{3+}$ formation), is faster with 50 mM $[B(cat)_2]^{-1}$ than with 50 mM TEA. TEA is observed to cause some reduction to $\mathbf{P}^{3+}$ prior to irradiation which can be problematic. This is significantly less of an issue with $[B(cat)_2]^{-1}$ as seen in Figures 2.8 and 2.9. Overall, we find that $[B(cat)_2]^{-1}$ is comparable and in many ways superior to TEA as a sacrificial donor. Because of ion-pairing, the k_q is larger than many common organic amines. Like organic amines, it rapidly decomposes such that the oxidation process is irreversible. Unfortunately, this irreversibility limits its usefulness for driving subsequent reactions.

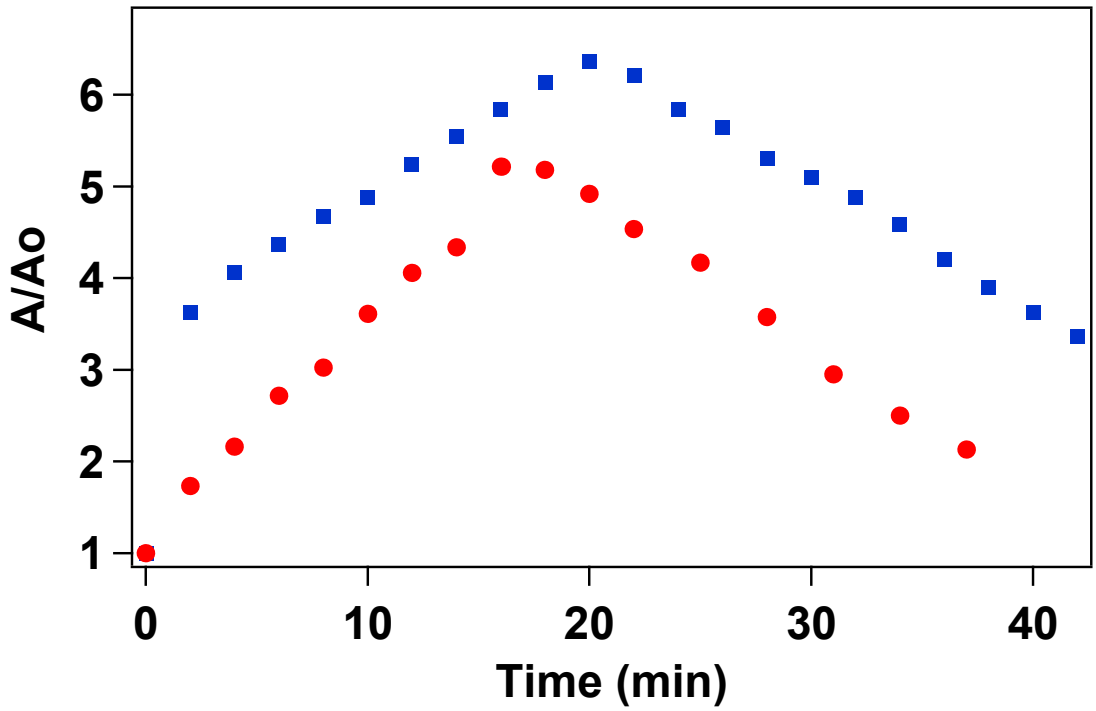

Figure 2.8 Reductive quenching of photoexcited complex $\mathbf{P}^{4+}$ in the presence of $[B(cat)_2]^-$ vs TEA as monitored by the appearance of the $\mathbf{P}^-$ (at 975 nm)
Conditions: (•) **P** (18.7 μM) and $[B(cat)_2]^-$ (50 mM) in degassed MeCN / 10 % water
(+) **P** (18.7 μM) and TEA (50 mM) in degassed MeCN / 10 % water
Irradiation: 100 W Tungsten bulb (360 nm cutoff) at 23°C for 45 minutes

The observed luminescence quenching of $[Ru(bpy)_3]^{2+}$ with $[B(cat)_2]^-$ was assumed to occur via electron-transfer; although, energy-transfer quenching could not be ruled out. The formation of $\mathbf{P}^{3+}$ with $[B(cat)_2]^-$ proves the quenching reaction involves electron transfer (reductive quenching) as energy transfer is unlikely to lead to the observed photoreaction.

2.3 Conclusion

The photochemical reactivity of the anionic complex, $[B(cat)_2]^-$, with $[Ru(bpy)_3]^{2+}$ was investigated. Stern-Volmer quenching studies in acetonitrile and 10% water/acetonitrile gave kq on the order of $3x10^6\ M^{-1}s^{-1}$. The quenching ability is strongly attenuated by increasing ionic strength supporting our hypothesis that ion-pairing plays an important role in the quenching reaction. Cyclic voltammetry shows two irreversible processes at 0.99 and 1.34 V (vs NHE) for $[B(cat)_2]^-$ which suggests that $[B(cat)_2]^-$ is unlikely to be useful as a reversible redox shuttle but instead may be useful as a sacrificial reductant. This was shown to be the case as $[B(cat)_2]^-$ can be used to photoreduce $\mathbf{P^{4+}}$ in 10% water/acetonitrile solution. This reactions also shows the quenching activity of $[B(cat)_2]^-$ is due to electron transfer quenching as opposed to energy transfer quenching. The ability of $[B(cat)_2]^-$ to ion-pair with $[Ru(bpy)_3]^{2+}$ and related chromophores can be shown to increase the efficiency of reductive quenching compared to neutral organic amines.

2.4 Experimental Section

2.4.1 Materials

1, 10-phenanthroline (phen), $RuCl_3$, 2, 2'-bipyridine, 1,2,4,5-benzenetetraamine, catechol and boric acid were purchased from Alfa and used as purchased. **P**$[PF_6]_4$ and $[N(CH_3)_4][B(cat)_2]$ were synthesized according to the literature[25, 35].

2.4.2 Instrumentation

^{1}H NMR spectra were obtained on Bruker MSL-300 spectrometer. Chemical shifts were given in ppm and referenced to TMS.

Cyclic voltammetry (CV) and differential pulse voltammetry (DPV) experiments were performed using a PC-controlled potentiostat (CH Instruments, electrochemical analyzer). Either glassy carbon (1.5 mm diameter disk) or Au (1.0 mm diameter disk) working electrodes from Cypress Systems were used. Immediately before use, the electrodes were polished to a mirror finish with wet alumina (Buehler, 0.05 *i*m), followed by rinsing with Millipore Milli-Q water, dried, and stored in acetonitrile during the preparation of the electrochemical cell. A Pt wire and a premium "no leak" Ag/AgCl reference electrode (Cypress, model EE009) were used as counter and reference electrodes, respectively, and potentials were quoted with respect to this reference. Experiments were conducted in dry acetonitrile (Aldrich, 99.93+%, HPLC grade) with 0.1 M $NBu_4^nPF_6$ (Sigma) as supporting electrolyte.

UV-vis spectrum was obtained on a Hewlett-Packard HP 8453A spectrophotometer in dry acetonitrile.

2.4.3 Photochemical studies

The stock solutions of **P**$[PF_6]_4$ (1.00 x 10^{-4} M) and$[N(CH_3)_4][B(cat)_2]$ (1.00 x 10^{-3} M) were prepared in acetonitrile (MeCN). A solution Ru complex, $\mathbf{P^{4+}}$, (19 μM) and $[B(cat)_2]^{-1}$ (50 mM) were sealed in a 3 ml glass cuvette. The mixture was degassed by bubbling N_2 for 10 minutes and the sample was placed in a water bath at 23°C. The sample was irradiated using 100 W tungsten bulb through 360 nm cutoff UV filter. The photon flux of 1.12 x 10^6 was obtained while placing the light source 3 cm away from the water bath. The sample was irradiated for 120 minutes and the UV spectra were recorded every 30 seconds. (HP 84353A UV-Vis system)

2.4.4 Rate Studies

The stock solutions of **P**$[PF_6]_4$ (1.00 x 10^{-4} M) and $[B(cat)_2]^{-1}$ (1.00 x 10^{-3} M) were prepared in dry MeCN. A typical photo-reduction experiment involves the preparation of 19 μM of **P** and 50 mM of $[B(cat)_2]^{-1}$ in MeCN. Mixtures of $\mathbf{P^{4+}}$ and $[B(cat)_2]^{-1}$ were placed in a sealed glass cuvette. In another cuvvette, 19 μM of $\mathbf{P^{4+}}$ and 50 mM of TEA in MeCN were sealed. The mixtures were degassed by bubbling N_2 for 10 minutes. The samples were placed in a water bath in order to maintain the temperature constant at 23°C. The sample was irradiated for 45 minutes with a 100 W tungsten bulb (photon flux of 1.12 x 10^6 and source to sample 3 cm) and the UV

absorption spectra were recorded every 30 seconds. The absorption-time plot of each sample was plotted.

2.4.5 Quenching of $[Ru(bpy)_3][PF_6]_2$ *with TEA and* $[B(cat)_2]^-$

A stock solution of $[Ru(bpy)_3][PF_6]_2$ (19 μM) was prepared in a 10% water-MeCN mixture. In addition, various concentrations of TEA and $[B(cat)_2]^-$ were prepared in a 10% water/MeCN mixture. After the mixture of $[Ru(bpy)_3]^{2+}$ and the sacrificial reducing agent were degassed by bubbling N_2 for 5 minutes, the emission absorbance of the mixture was recorded. The Absorption-concentration plot of each sacrificial reducing agent was plotted.

CHAPTER 3

ELECTROCHEMICAL AND PHOTOCHEMICAL REDUCTION OF $[(phen)_2Ru(dppz)\text{-}(dppz)Ru(phen)_2]^{4+}$ DIMER

3.1 Introduction

Ruthenium polypyridyl compounds have been extensively studied for applications in solar energy conversion because they exhibit both long-lived photoexcited states and favorable energetics. The excited-state lifetime can be tuned by electronic and structural changes on the coordinating ligands. Ligand delocalization and rigidity increase the excited state lifetime but often decrease the energy gap between the excited and ground state.[34-37] Typically, the metal center strongly interacts with the low-lying π* orbitals on the aromatic ligand via dπ-pπ bonding and photoexcitation formally results in a metal to ligand charge transfer (MLCT). Among the flat aromatic ligands, dipyrido[3,2-a: 2', 3'-c] phenazine (dppz) has drawn a lot of interest because of the weak electronic coupling of the phenazine-based LUMO and the Ru(II) ion. Instead, the strongest electronic transition observed for Ru-dppz complexes is a Ru(II)-'bpy-like' MLCT which involves the 'bpy-like' LUMO+1 as the dominant acceptor orbital.[38]

De Cola and co-workers have reported the electrochemical and redox properties of a Ru(II) dimer with the bridging bdppz ligand, where bdppz stands for 1,19-dipyrido[3,2-*a*:29,39-*c*]phenazin-1,19-yldipyrido[3,2-*a*:29,39-*c*]-phenazine.[36] The cyclic voltammogram of the complex $[(phen)_2Ru(bdppz)Ru(phen)_2]^{4+}$ (**1^{4+}**) reveals two sequential, one electron reductions at -0.683 V and -0.873 V vs NHE, respectively. These first two reductions are localized on the phenazine portions of the bdppz ligand, much like the acceptor capabilities of the tatpp ligand in complex **P^{4+}**. However, the first and second reduction potentials of **1^{4+}** are significantly more negative than those found in **P^{4+}** (as shown in Table 3.1) and thus complex **1^{4+}** has the potential to store more reducing energy per electron than **P^{4+}**. While De Cola and coworkers reported on the electrochemical and chemical reduction of complex **1^{4+}**, they did not investigate its photochemistry. We decided to investigate the photoreduction of **1^{4+}** under conditions that proven so successful for the related complex **P^{4+}**. It was our hope that we could doubly-reduce complex **1^{4+}** under photochemical conditions and use these reducing electrons to generate H_2 under appropriate conditions. The important redox and protonation states of $[(phen)_2Ru(bdppz)Ru(phen)_2]^{4+}$ are shown in scheme 1.

Table 3.1 First and second reduction potentials of **P^{4+}** and **1^{4+}** vs NHE[24, 35]

$P^{4+} \rightarrow P^{3+}$	**$P^{3+} \rightarrow P^{2+}$**	**$1^{4+} \rightarrow 1^{3+}$**	**$1^{3+} \rightarrow 1^{2+}$**
-0.023 V	-0.513 V	-0.683 V	-0.873 V

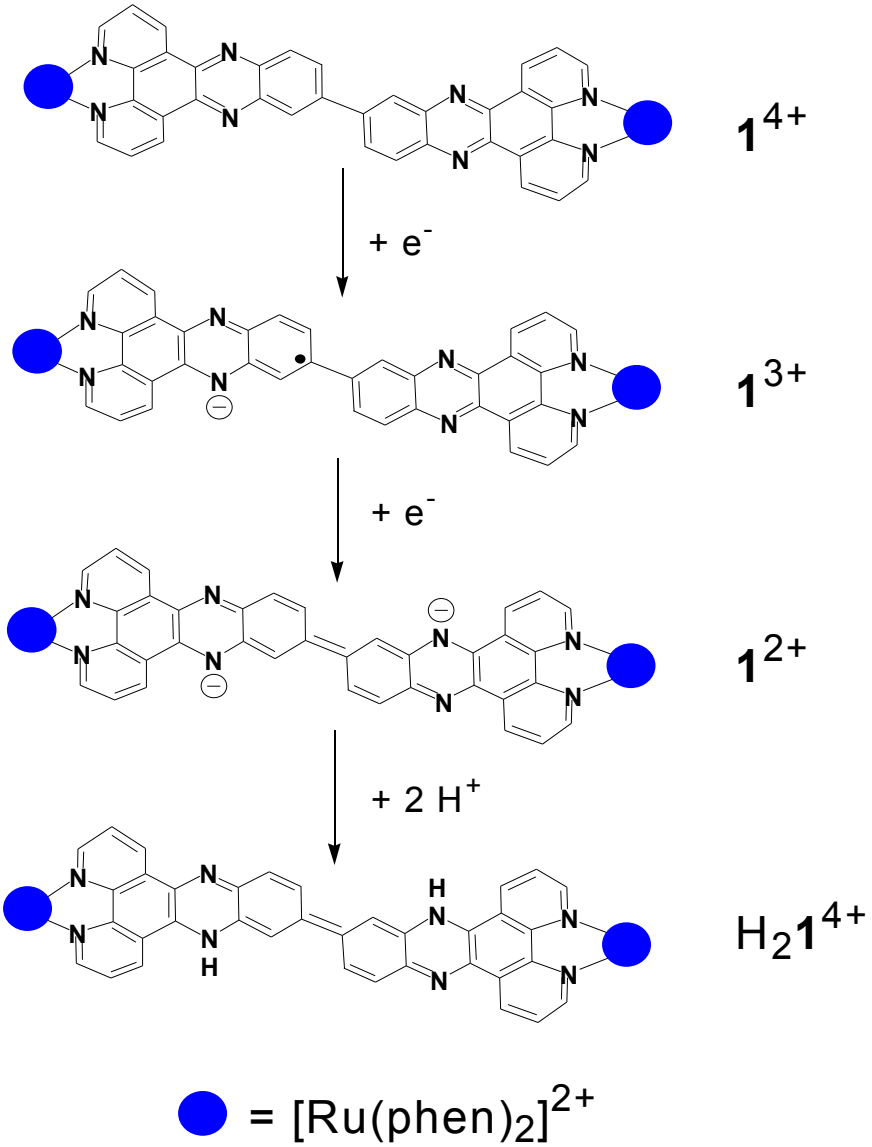

Scheme 3.1 Redox States of $\mathbf{1}^{4+}$

3.2 Results and Discussion

3.2.1 Electrochemical Reduction and Protonation of $\boldsymbol{1^{4+}}$

The electrochemical reduction and UV-vis absorption spectra of $\mathbf{1^{4+}}$ have been studied by De-Cola and coworkers.[34] The UV-vis absorption spectra of the $\mathbf{1^{4+}}$ undergoes major changes when it is reduced stepwise to $\mathbf{1^{2+}}$ in a spectroelectrochemical cell (OTTLE cell) as seen in Figure 3.2 a**.** The characteristic absorption band of the $\mathbf{1^{4+}}$ at 407 nm diminishes upon reduction to $\mathbf{1^{3+}}$. A new absorption band of one electron reduced $\mathbf{1^{3+}}$ is observed around 580 nm which can be related to the intraligand charge transfer(IL) transition of the radical $[bdppz]^{\cdot-}$ ligand. When the complex is further reduced to $\mathbf{1^{2+}}$**,** a new band arises at 965 nm which corresponds to the IL transition of the new delocalized phenazine moiety. When the negatively charged phenazine units are protonated, an absorption band of the product $\mathbf{H_2 1^{4+}}$ appears at 650 nm as shown in Figure 3.2 b.

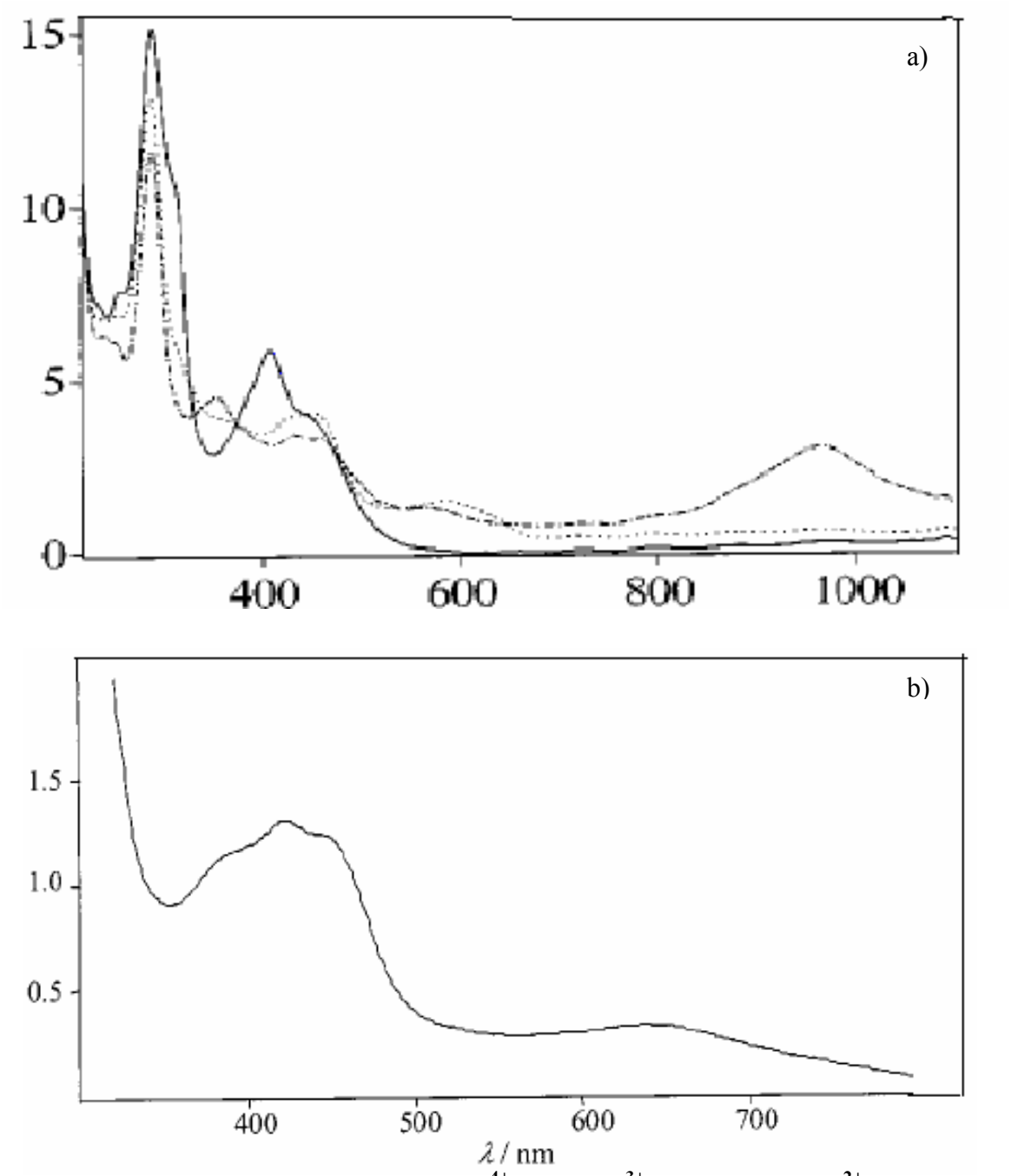

Figure 3.2 a) UV/Vis spectra of $\mathbf{1}^{4+}$ (——), $\mathbf{1}^{3+}$ **(·····)** and $\mathbf{1}^{2+}$ **(— · · —)** in butyronitrile/ 0.3 M Bu_4NPF_6, recorded in an OTTLE cell

b) UV/Vis spectra of $\mathbf{H_2 1}^{4+}$ chemical reduction with Zn in deaerated acidified acetonitrile[34]

3.2.2 Chemical Reduction and Protonation of $\mathbf{1}^{4+}$

As seen in reactions 1 and 2, the singly ($\mathbf{1}^{3+}$) and doubly ($\mathbf{1}^{2+}$) reduced forms of $\mathbf{1}^{4+}$ are generated in situ via stoichiometric reductions with cobaltocene in acetonitrile, and their absorption spectra are shown in Figure 3.3. Cobaltocene is a strong one-electron reducing agent (-0.795 V vs NHE in acetonitrile[23]) and it is thermodynamically capable of generating $\mathbf{1}^{3+}$ (**(**$E_{1/2}$ of -0.683 V vs NHE**).** The doubly reduced species $\mathbf{1}^{2+}$ is generated upon addition of an excess of cobaltocene. The oxidized cobaltocenium ion produced is light yellow in color and adds no appreciable absorption to the visible and near-IR portion (350-1100 nm) of the absorption spectra.

$$1^{4+} + Co(Cp)_2 \longrightarrow 1^{3+} + Co(Cp)_2^{+} \qquad (1)$$

$$1^{4+} + 2\ Co(Cp)_2 \longrightarrow 1^{2+} + 2\ Co(Cp)_2^{+} \qquad (2)$$

As expected from De Cola's work, both $\mathbf{1}^{3+}$ and $\mathbf{1}^{2+}$ show new, strong ligand-centered (LC) bands in the visible and near-IR portion of the spectrum. Addition of one equivalent cobaltacene results in an immediate color change of the solution from brown to green which corresponds to a new absorption band at 585 nm for $\mathbf{1}^{3+}$. Addition of excess (almost three equivalents) of cobaltacene generates $\mathbf{1}^{2+}$ and results small decrease in the peak at 585 and broad band grows at 950 nm.

The presence of protons alters the absorption spectrum as seen here by reduction of $\mathbf{1}^{4+}$ to $H_2\mathbf{1}^{4+}$ with sodium borohydride ($NaBH_4$). As seen in Figure 3.4, we observed two broad peaks around 620 nm and 800 nm for the new complex, $H_2\mathbf{1}^{4+}$. De Cola and

coworkers showed that reduction by zinc metal in the presence in HCl gives the same species, $H_2\mathbf{1}^{4+}$.

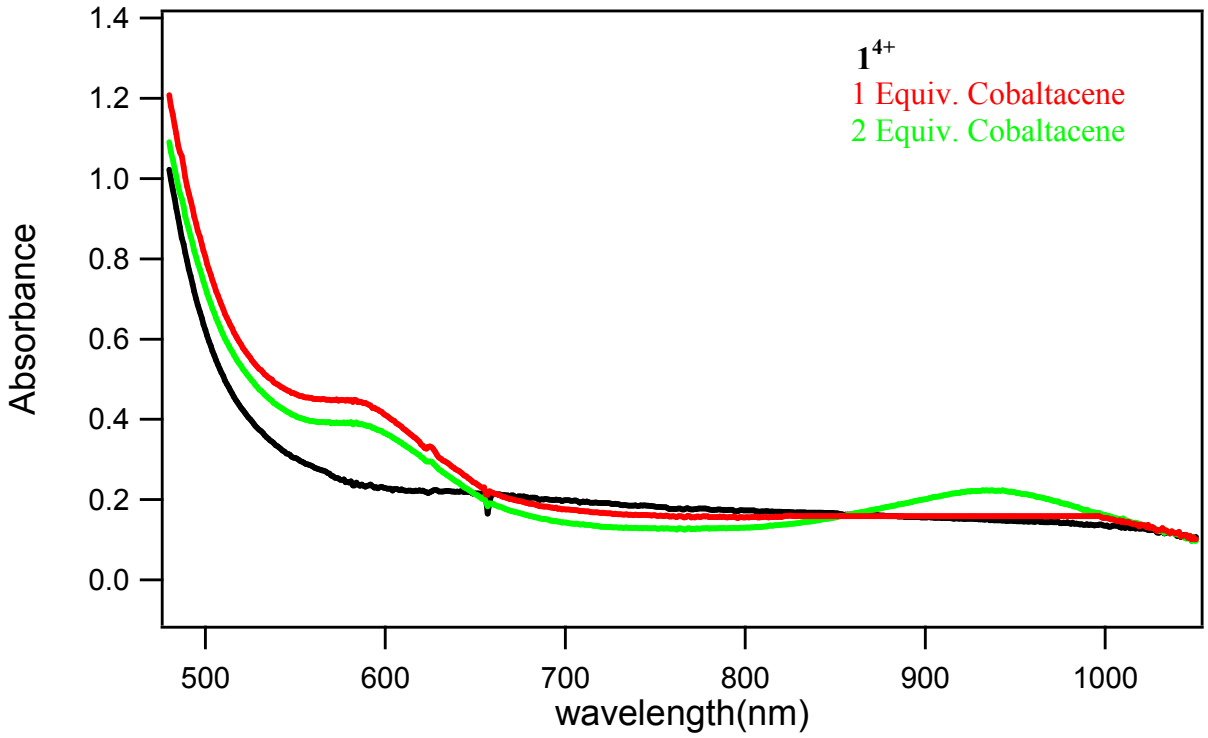

Figure 3.3 Absorption spectra of $\mathbf{1}^{4+}$ (black), $\mathbf{1}^{3+}$ (red) and $\mathbf{1}^{2+}$ (green) in acetonitrile as generated in situ via stoichiometic reductions with $Co(Cp)_2$

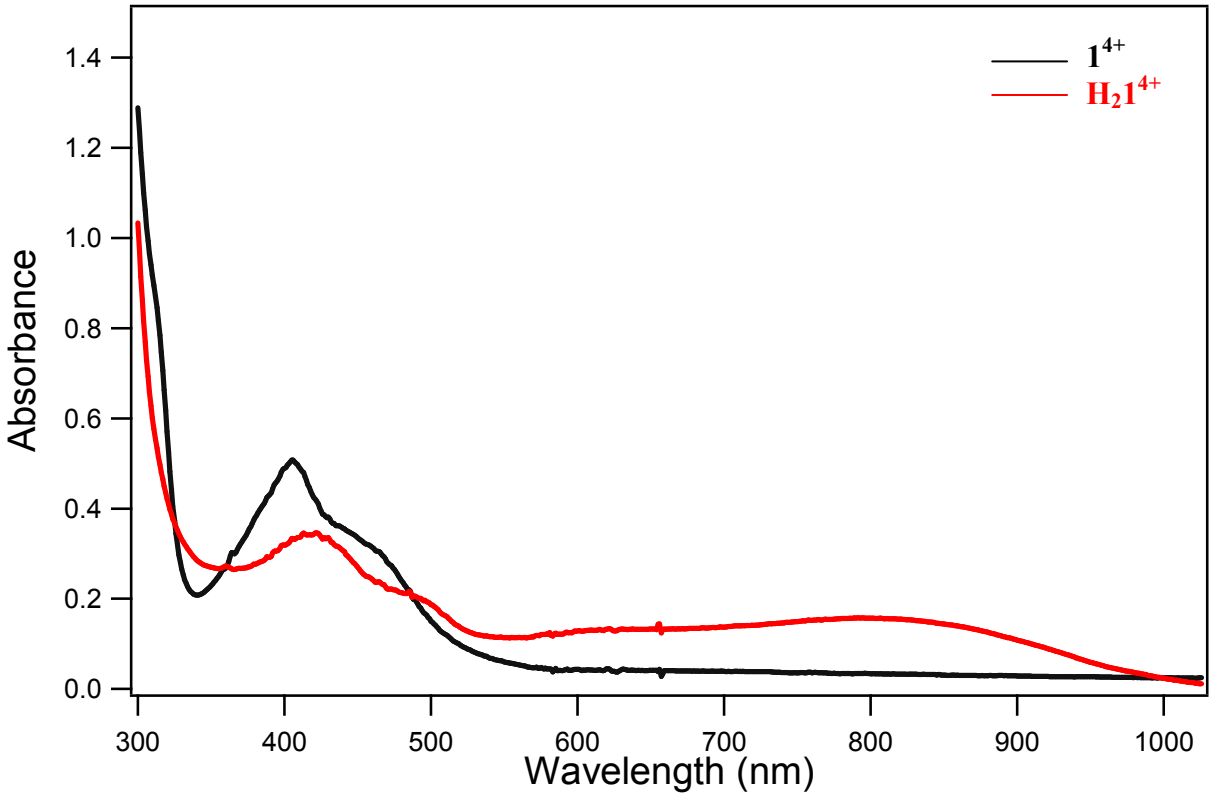

Figure 3.4 Chemical reductions of $\mathbf{1}^{4+}$ using sodium borohydride in 5 % water/ MeCN

3.2.3 Photochemical Reduction of $\boldsymbol{1}^{4+}$ *with TEA*

Photochemical reduction of $\mathbf{1}^{4+}$ was carried out in MeCN with both triethylamine (TEA) and triethanolamine (TEOA) as sacrificial reducing agents. When the sample is irradiated with visible light, the color of the solution slowly changes from brown to green. As seen in Figure 3.5a, the color change is associated with the appearance of a new band at 580 nm which shows formation of $\mathbf{1}^{3+}$. However as seen in Figure 3.5b, continued irradiation eventually leads to a small decrease in intensity for the broad peak at 580 nm; however, no further changes are observed in the absorption

spectra. Finally, if the irradiated sample is exposed to air, the initial spectrum is rapidly regenerated.

When the photoirradiation experiment was performed in water instead of MeCN, virtually identical spectral changes were observed. As seen in Figure 3.6, the appearance of a broad peak at 580 nm is observed first indication formation of $\mathbf{1}^{3+}$**.** Subsequently, this peak diminishes somewhat in intensity; however, there is no indication of further reduction as this would be expected to give a new absorption between 700 and 950 nm.

In conclusion, the Ru complex $\mathbf{1}^{4+}$ undergoes a single photochemical reduction to $\mathbf{1}^{3+}$ under conditions that lead to multiple reductions for the related $\mathbf{P}^{4+}$ complex. The reduction is localized on the bdppz ligand and is likely localized in a 'phenazine-like' acceptor orbital.

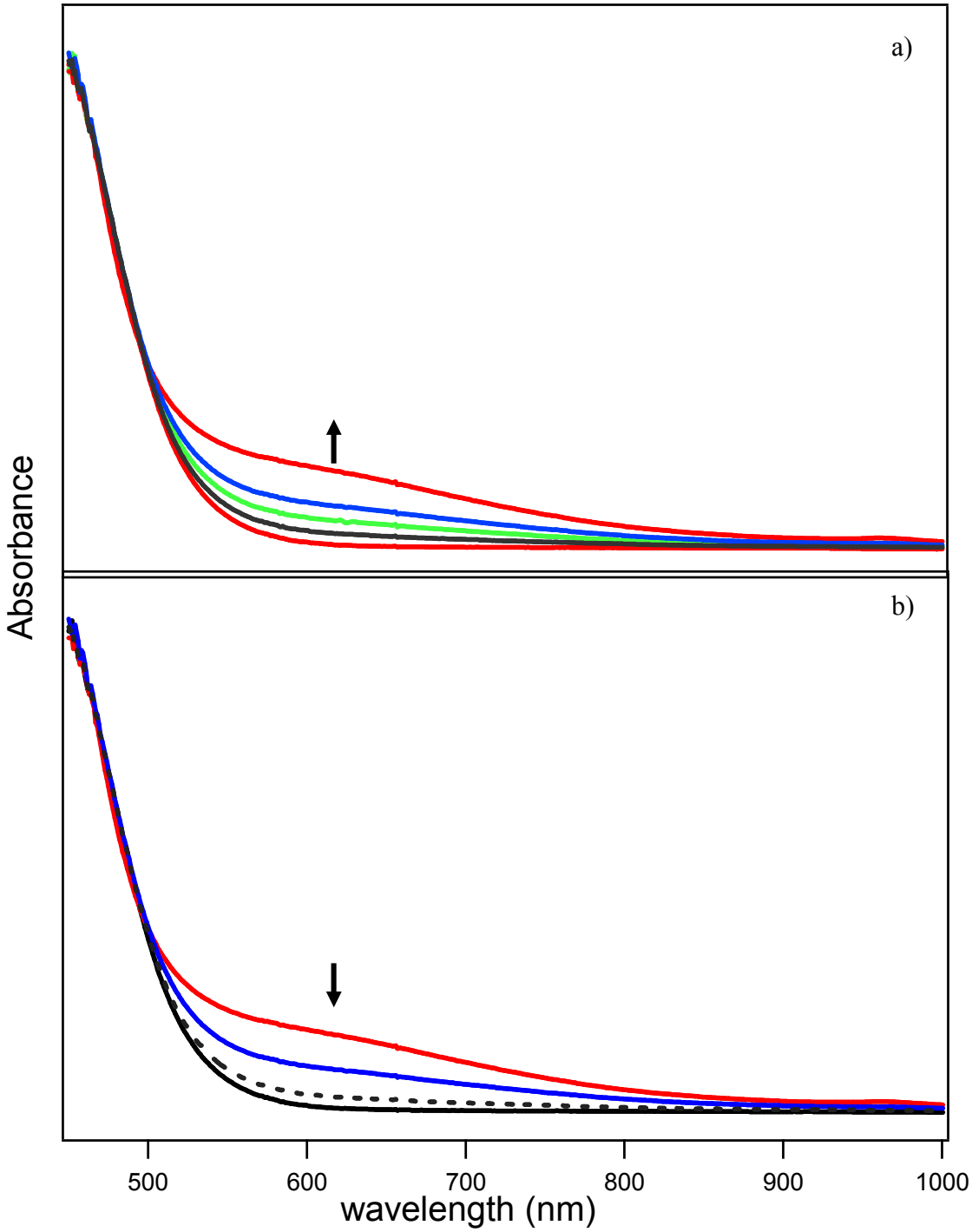

Figure 3.5 The visible spectrum of $\mathbf{1}^{4+}$ (19 μM) in the presence of 0.3 M TEA in degassed acetonitrile during photoirradiation [100 W tungsten bulb (light source), 360 nm cutoff filter] a) 0-15 minutes b) 15-60 minutes (red to blue). Black dashed line shows final spectrum after exposure to O_2.

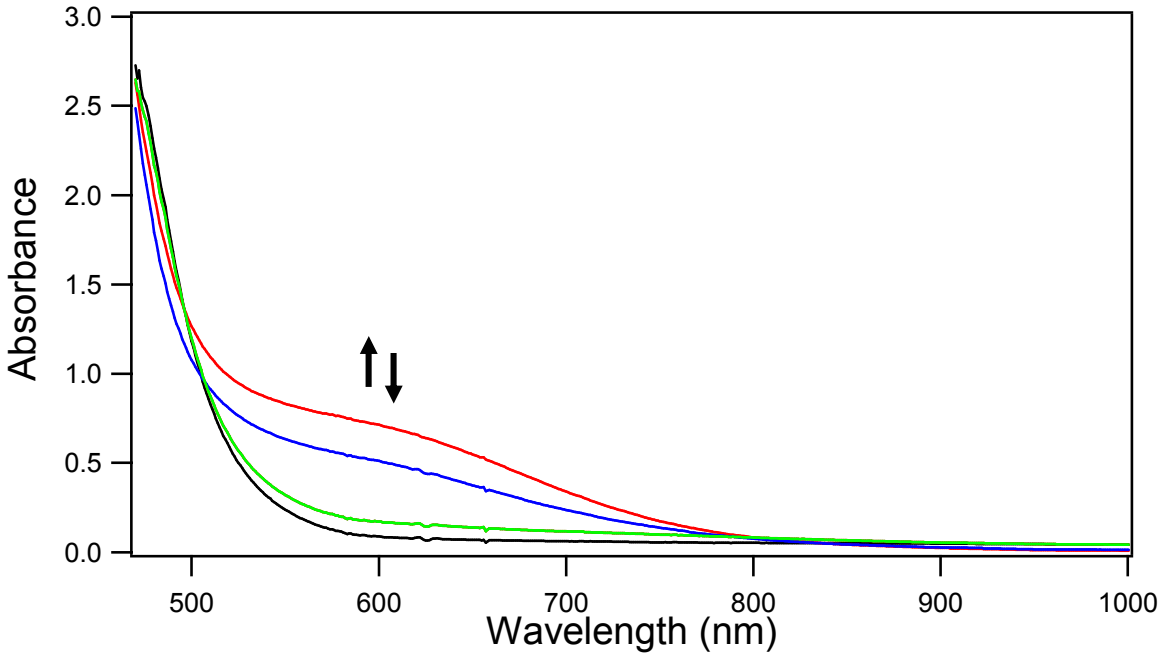

Figure 3.6 The visible spectrum of $\mathbf{1}^{4+}$ (18.7 μM) in the presence of 0.3 M TEOA in degassed water during photoirradiation[100 W tungsten bulb (light source), 360 nm cutoff filter]

3.3 Experimental Section

3.3.1 Photochemical Studies

The stock solution of $[(phen)_2Ru(bdppz)Ru(phen)_2][PF_6]_4$[29] (**$1^{4+}$**, 1.00 x 10^{-4} M) was prepared in MeCN. From this stock a solution 19 μM in **1^{4+}** and 0.32 M in TEA was prepared in a sealed 3 mL glass cuvette. The solution was degassed by gently bubbling N_2 through it for 10 minutes. The sample was placed in a water bath at 23°C and irradiated with a 100 W tungsten bulb through 360 nm cutoff UV filter. The photon flux of 1.12 x 10^6 was obtained while placing the light source 3 cm away from the water bath. The sample was irradiated for 60 minutes, and the UV spectra are recorded every 30 seconds. The experiment was repeated with triethanolamine (TEOA) in place of the TEA.

*3.3.2 Chemical reductions of **1^{4+}** with $Co(Cp)_2$*

All redox and protonation titrations were carried out in a nitrogen atmosphere glove box. Stock solutions of **1^{4+}** (1.00 x 10^{-4} M), $Co(Cp)_2$ (10.00 x 10^{-3} M) and TFA (0.013 M) were prepared in degassed acetonitrile. **1^{3+}** and **1^{2+}** were generated by adding one and two equivalents of $Co(Cp)_2$ respectively. Since the cobaltocene does not have enough potential to form doubly reduced species, almost three equivalents of $Co(Cp)_2$ were added in order to form **1^{2+}.** The doubly reduced, doubly protonated species, **$H_2 1^{4+}$**, were generated by adding 10 μL of 0.5 M $NaBH_4$ (in diethoxy ether) to a 19 μM **1^{4+}** solution in MeCN.

APPENDIX A

THE UV-VIS SPECTRUM OF $\mathbf{P}^{4+}$ IN THE PRESENCE OF $[B(cat)_2]^-$

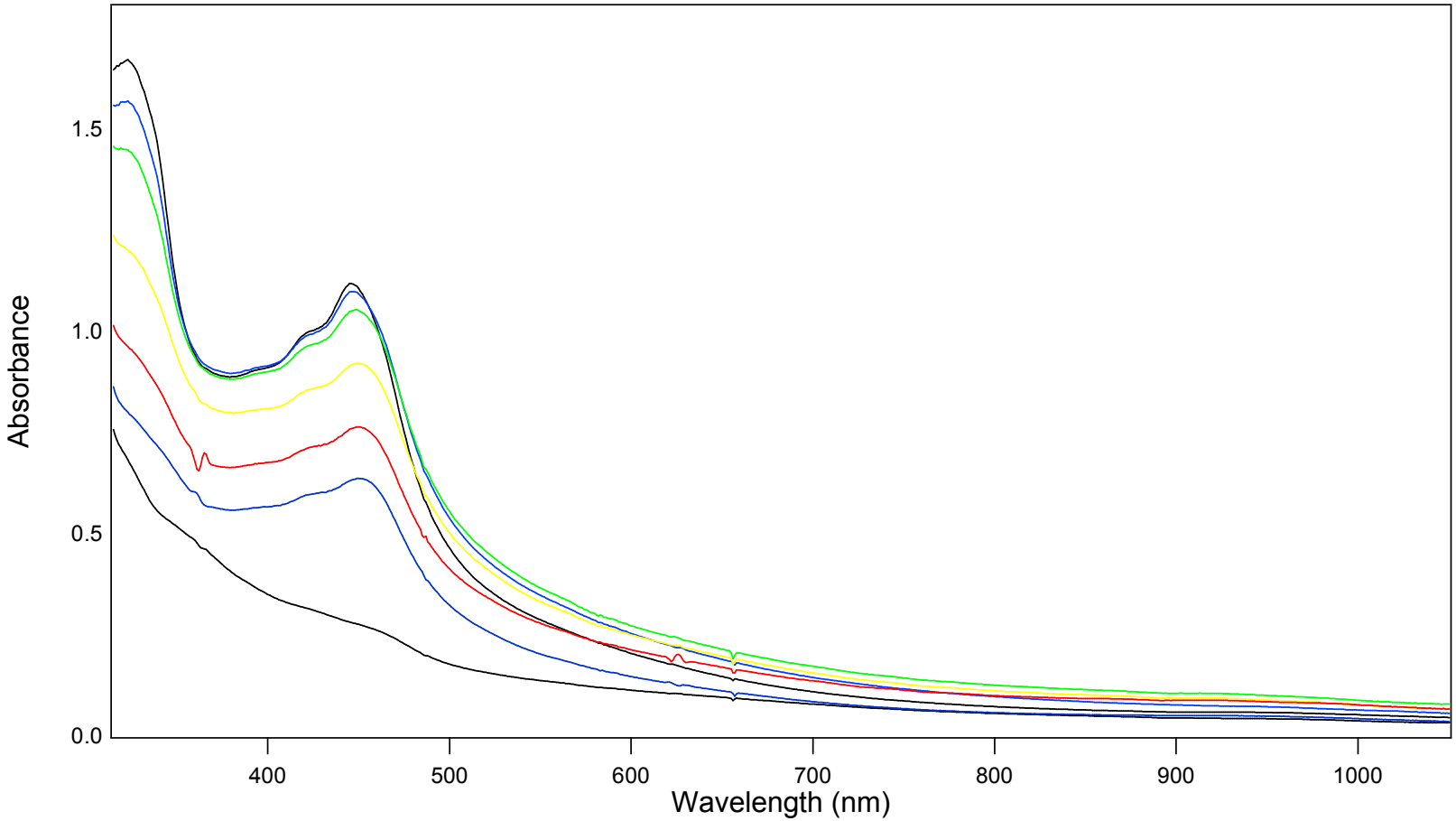

Figure A.1 The visible spectrum of $\mathbf{P}^{4+}$ (18.7 μM) in the presence of 50 mM of $[B(cat)_2]^-$ in degassed MeCN during photoirradiation [100 W tungsten bulb (light source), 360 nm cutoff filter] The brown precipitation occurs.

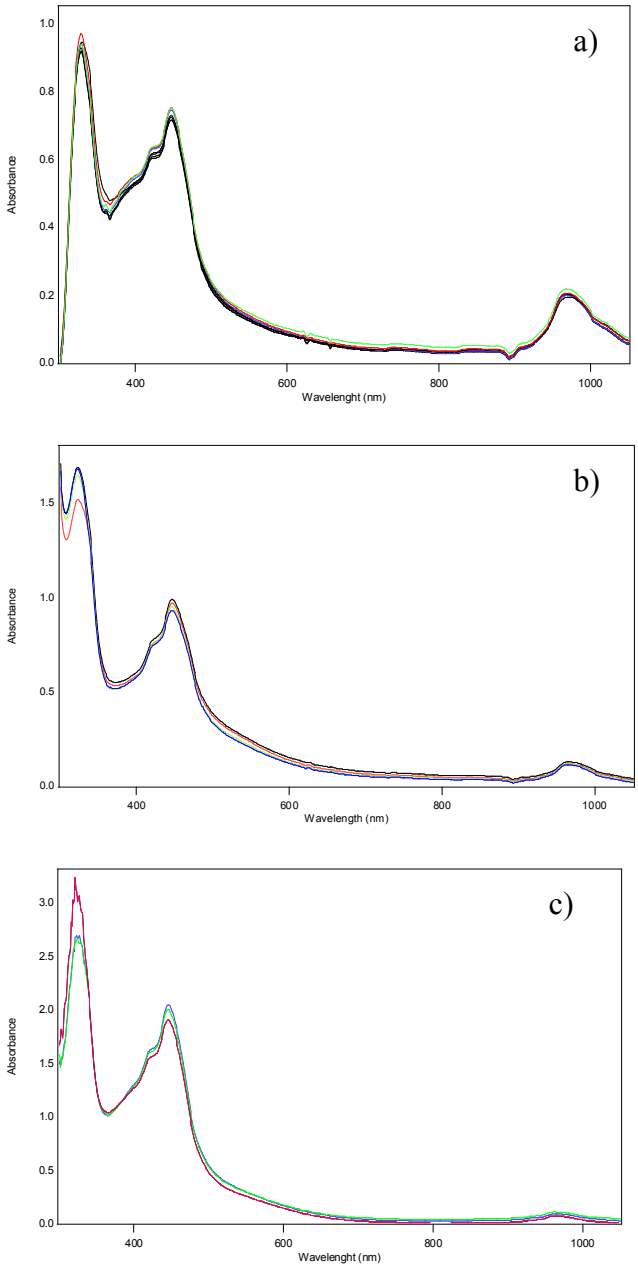

Figure A.2 The visible spectrum of $\mathbf{P^{4+}}$ (18.7 µM) in the presence 50 mM of $[B(cat)_2]^-$ in degassed MeCN and 0.01 M HCl during photoirradiation [100 W tungsten bulb (light source), 360 nm cutoff filter] at different acidic mediums. a) $pH_m = 2.51$ b) $pH_m = 4.13$ c) $pH_m = 6.07$

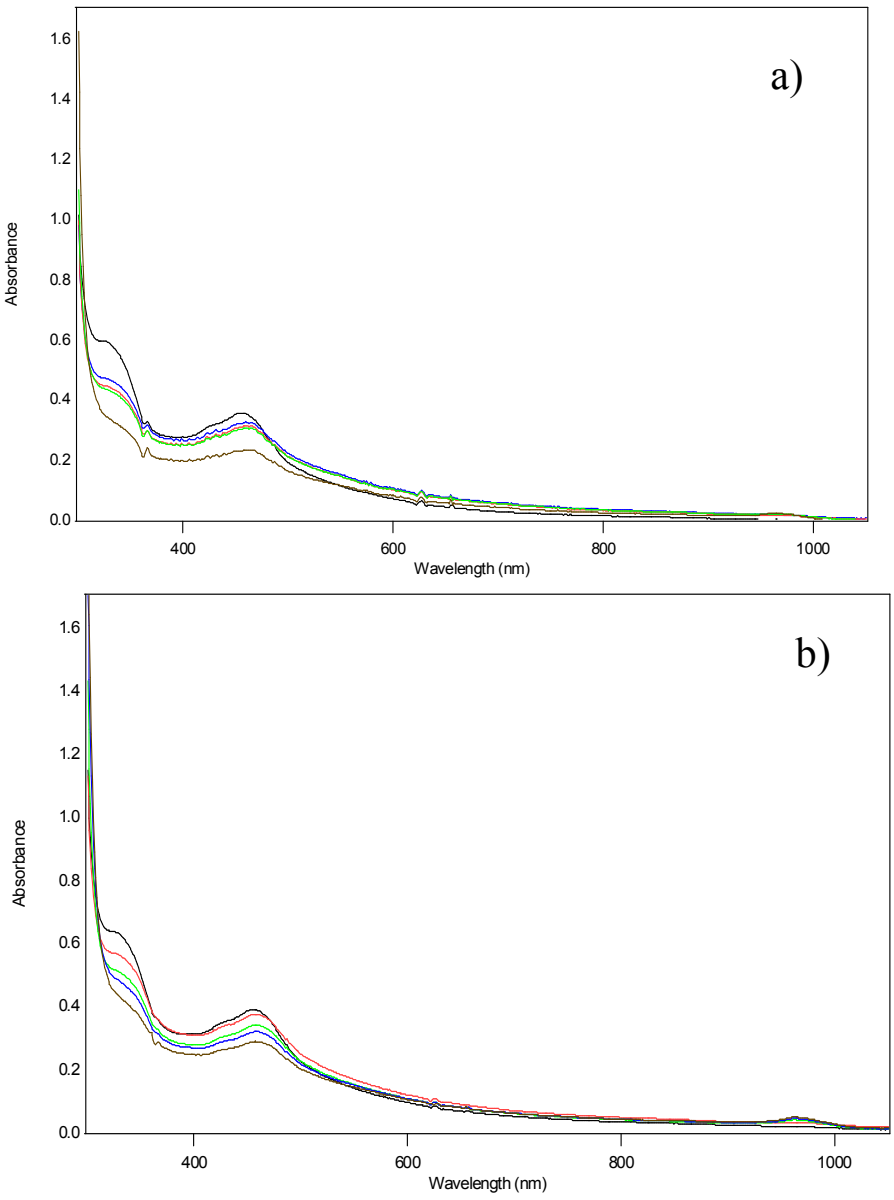

Figure A.3 The visible spectrum of $\mathbf{P}^{4+}$ (18.7 μM) in the presence 50 mM of $[B(cat)_2]^-$ in degassed water and 0.01 M NaOH during photoirradiation [100 W tungsten bulb (light source), 360 nm cutoff filter] at different acidic mediums. a) $pH_m = 8.04$ b) $pH_m = 8.97$

APPENDIX B

SYNTHESIS SCHEME AND METHODS OF $[B(cat)_2]^{-1}$, $\mathbf{P}^{4+}$ AND $\mathbf{1}^{4+}$

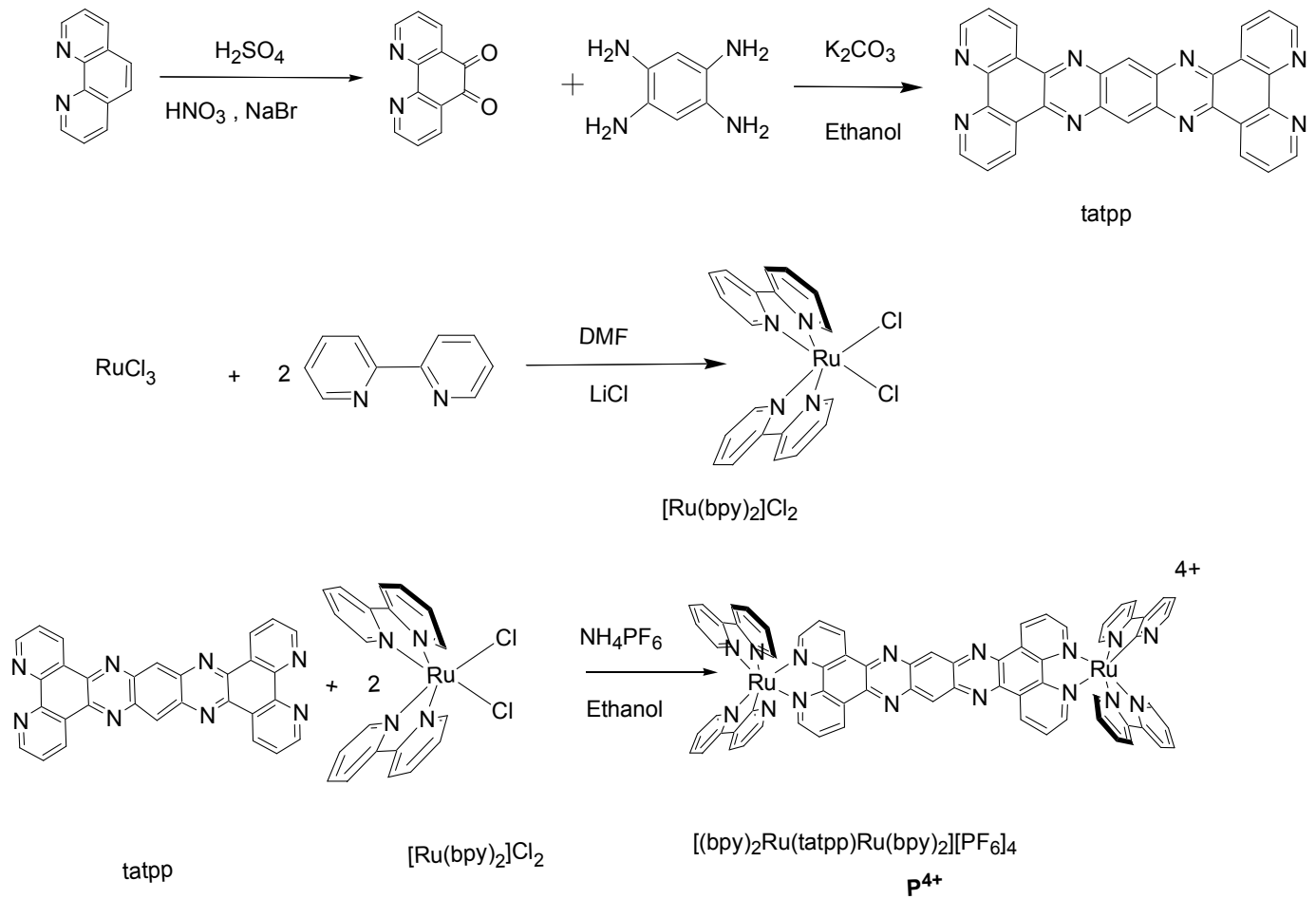

Scheme B.1 Synthesis of $\mathbf{P^{4+}}$

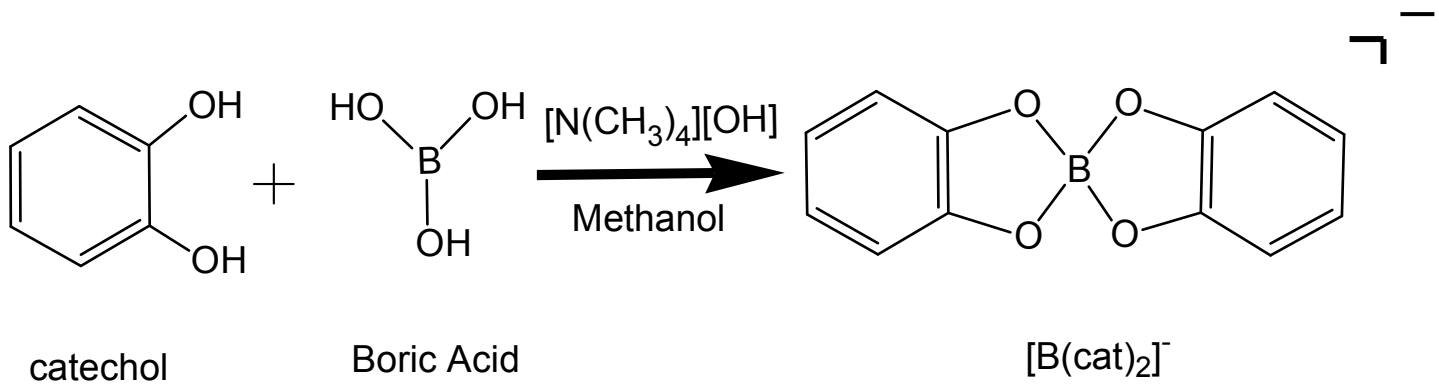

Scheme B. 2 Synthesis of [[B(cat)$_2$]$^-$

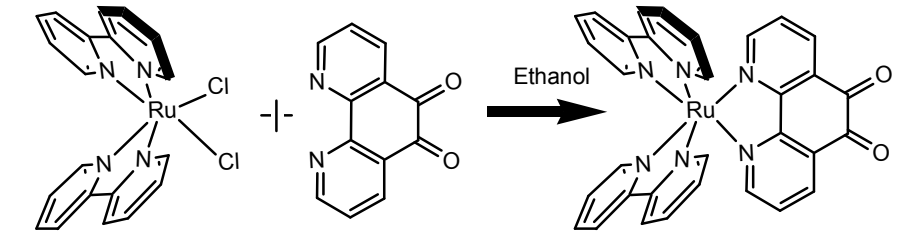

$[Ru(bpy)_2]Cl_2$ 1, 10 phenanthroline 5, 6 dione $[Ru(phen)_2phendione][PF_6]$

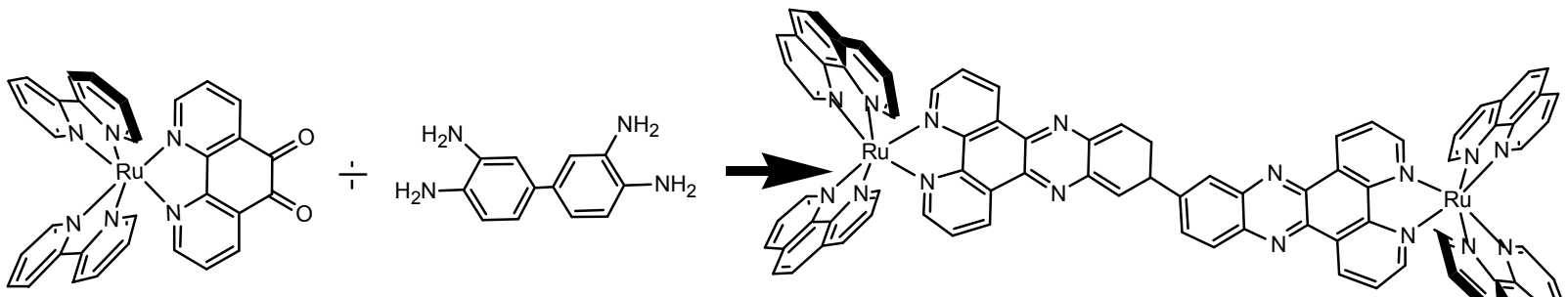

$[Ru(phen)_2phendione][PF_6]$

3, 3 diaminobenzidine

1^{4+}

Scheme B.3 Synthesis of $\mathbf{1}^{4+}$

Synthesis:

Chemicals: The compound 1, 1o phenanthroline(phen), 1, 2, 4, 5 benzenetetraamine tetrahydrochloride, hydrated Ruthenium(III) chloride, boric acid and catechol are purchased from Aldrich and used as recieved. All of the solvents are reagent grade and used as received. The compound 1, 10 phenanthroline 5, 6-dione[39], $[Ru(bpy)_2]Cl_2$[40] 9,11,20,22-Tetraazatetrapyrido[3,2-a:2'3'-c:3'',2''-l:2''',3'''-n]pentacene (tatpp)[25], $[(bpy)_2Ru(tatpp)Ru(bpy)_2][PF_6]_4$[25] and $[B(cat)_2][N(CH_3)_4]$[35] were synthesized according to literature procedure.

1, 10 phenanthroline 5,6-dione. A mixture of 1,10 phenanthroline 5,6-dione (5.00 gr, 0.025 mo) and NaBr(2.50 gr, 0.025 mol) was suspended in a mixture of H_2SO_4(conc.) and HNO_3(70%) and refluxed for an hour. After cooling of the reaction to the room temperature, the pH was adjusted to 6 while adding NaOH (125ml, 10 M). After extracting phendione with CH_2Cl_2 (3x), the resulting compound left in the fridge overnight. After the precipate filtered out, the compound dried in vacuo at 60°C.Yield: 3.45 g (60.2 %) ^{1}H NMR (δ, 300 MHz, MeCN-d_6): 8.95 Hz (d,J) 2H, 8.40 Hz (d,J) 2H, 7.65 Hz (dd,J) 2H.

$[Ru(bpy)_2]Cl_2$: A mixture of $RuCl_3.H_2O$ (2.50 g, 8.100 mmol), 2-2' biprydine (3.01 g, 19.1 mmol) and LiCl (2.750 g, 6.41 mmol) was suspended in DMF and refluxed overnight. After cooling of the reaction to the room temperature, acetone added to the solution and kept at 10°C overnight. After washing crystals with water (3x), the crystals

dried vith vacuo at 60^0C. Yield 3.31 g (85.2%). (δ, 300 MHz, DMSO-d_6): 9,95 Hz (d,2H), 8.65 Hz (d, 2H), 8.48 Hz (d, 2H), 8.05 Hz (dd, 2H), 7.75 Hz (dd, 2H), 7.65 Hz (dd, 2H), 7.50 Hz (d, 2H), 7.10 Hz (d, 2H).

9,11,20,22-Tetraazatetrapyrido[3,2-a:2'3'-c:3'',2''-l:2''',3'''-n]pentacene (tatpp). A mixture of phendione (0.40 g, 1.91 mmol), 1,2,4,5-benzenetetramine tetrahydrochloride (0.27 g, 0.95 mmol), and potassium carbonate (0.26 g, 1.91 mmol) was suspended in ethanol (15 mL) and refluxed under nitrogen for 12 h. After cooling of the reaction to room temperature, the precipitate was filtered out, washed with 15 mL of hot water (3x) and 15 mL of boiling ethanol (3x), and dried in vacuo at 60 °C. Yield: 0.32g (70.1 %). ^{1}H NMR (300 MHz, MeCN-d_6) 90:10; δ, ppm): 10.20 (d, J = 8.0 Hz, 4H), 9.79 (s, 2H), 8.33 (d, J = 4.0 Hz, 4H), 8.36 (dd, J_1 = 7.3 Hz, J_2 = 4.5 Hz, 4H).

$[(bpy)_2Ru(tatpp)Ru(bpy)_2][PF_6]_4$. A mixture of tatpp (0.806g, 0.016 mmol) and $Ru(bpy)_2Cl_2$ (0.403 g, 0.075 mmol) was suspended in ethanol (30 mL) and water (30 mL) and refluxed for 7 days under N_2 atmosphere. After reflux, the solution was allowed to stand for 12 h at 4 °C. The solution was filtered and the product precipitated by addition of aqueous NH_4PF_6 to the supernatant. The precipitate was filtered out and washed with 10 mL of water (3x) and 10 mL of ethanol. The crude product was further purified by repeated (3x) metatheses between the Cl^- and PF_6^- salts. The chloride salt was prepared from the hexafluorophosphate salt by dissolving the dried complex in a minimum amount of acetone and adding a concentrated solution of Bu_4NCl in acetone.

The resulting precipitate was filtered out and washed with 5 mL of acetone (3x) and 10 mL of diethyl ether. The hexafluorophosphate salt was prepared from the chloride form by dissolving the complex in a minimum amount of water and adding a concentrated solution of ammonium hexafluorophosphate. The resulting precipitate was filtered out and washed with 10 mL of water (3x), 10 mL of ethanol, and 10 mL of diethyl ether. Yield (PF_6^- salt): 0.273 g (65.2 %). ^{1}H NMR (δ, 300 MHz, MeCN-d_6): 9.70 (d, J = 8.3 Hz, 4H), 8.65 (dd, J_1 = 2.8 Hz, J_2 = 8.3 Hz, 8H), 8.30 (d, J = 5.0 Hz, 4H), 8.30 (s, 8H), 8.26 (s, 2H), 8.15 (d, J = 5.5 Hz, 4H), 8.03 (d, J = 5.5 Hz, 4H), 7.82 (dd, J_1 = 7.8 Hz, J_2 = 5.5 Hz, 4H), 7.72 (dd, J_1 =8.3 Hz, J_2 = 5.1 Hz, 4H), 7.66 (J_1 = 8.3 Hz, J_2 = 5.5 Hz, 4H).

[N(CH$_3$)$_4$][B(cat)$_2$.]. Catechol (2.03g, 18.18 mmol) and boric acid (0.56g, 9.03 mmol) were dissolved in MeOH and 10% tetramethylammonium hydroxide and water mixture. After stirring for 20 minutes, the solvent evaporated until the white precipitation occurs. The precipitation was washed with MeOH and isopropyl alcohol and the white crystals formed with addition of ether. Yield: 1.609 g (78.3 %). ^{1}H NMR (δ, 300 MHz, MeCN-d_6): 3.00 Hz 6.78 (dd, J=6.63, 2H), 6.70 Hz (dd, J= 6.45, 2H)

APPENDIX C

^{1}H NMR of "P^{4+}", "1^{4+}" AND $[B(cat)_2]^-$

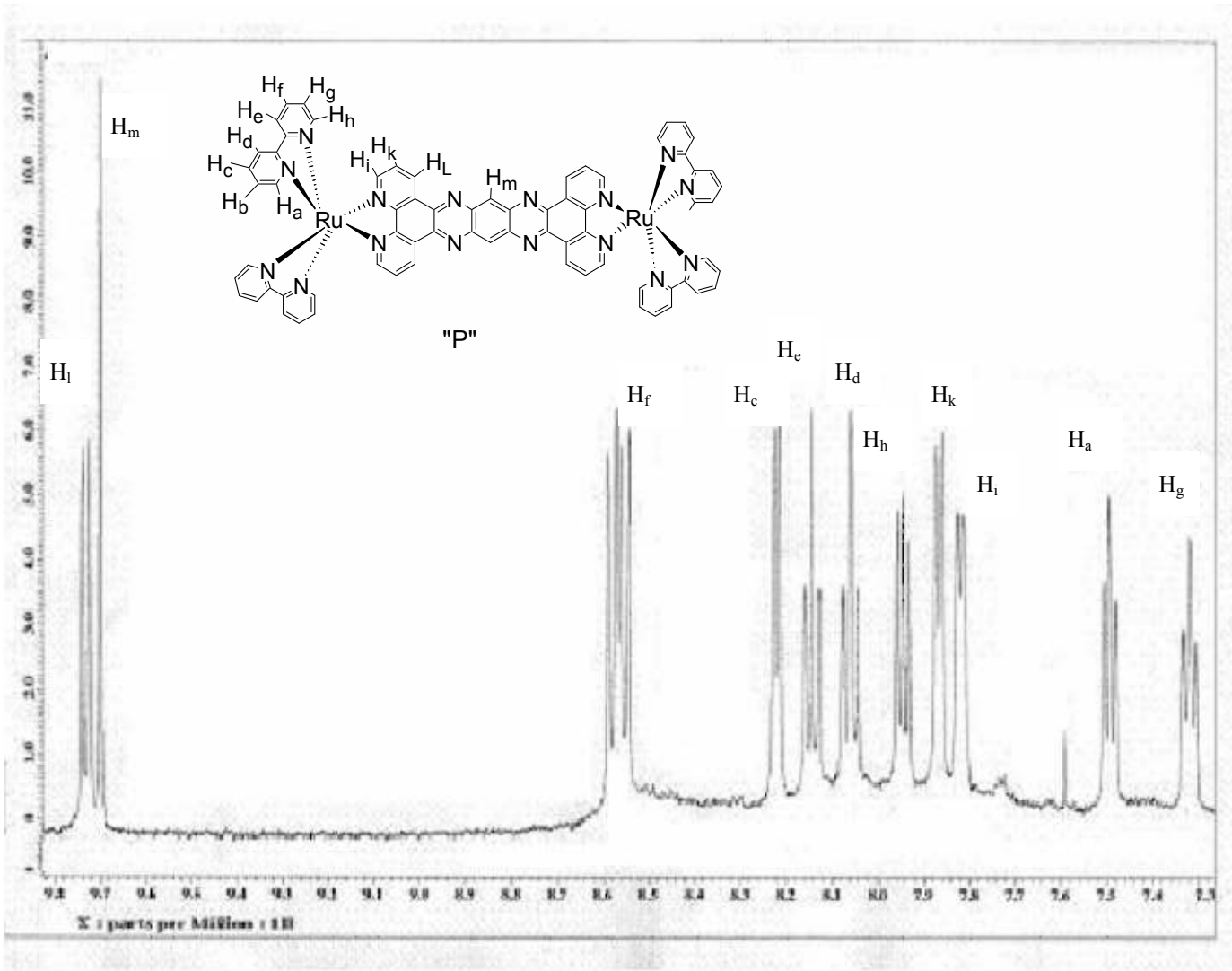

Figure C.1 ^{1}H NMR of $\mathbf{P^{4+}}$, 300 MHz, MeCN-d_6

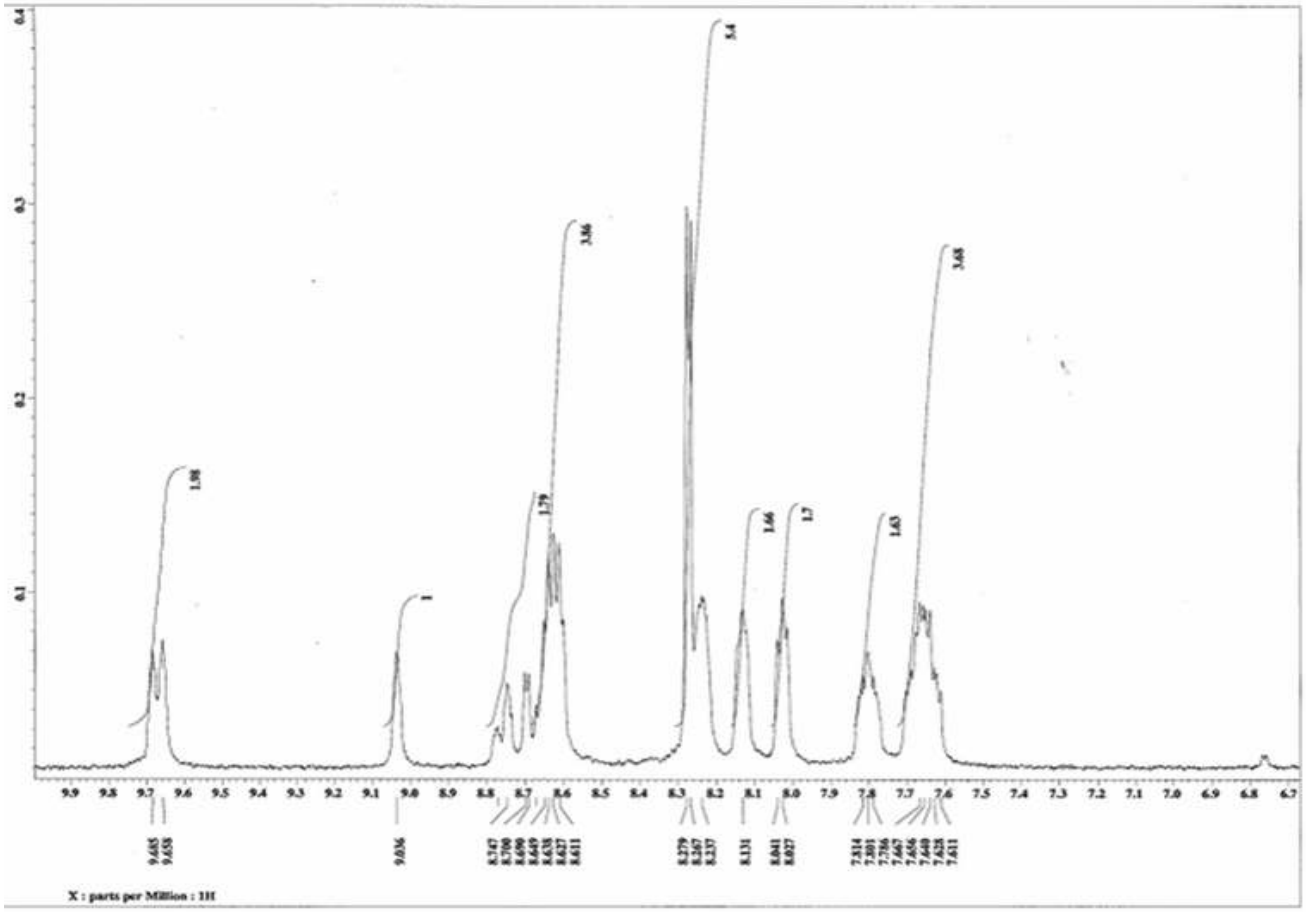

Figure C.2 ^{1}H NMR of $\mathbf{1}^{4+}$, 300, MeCN-d_6

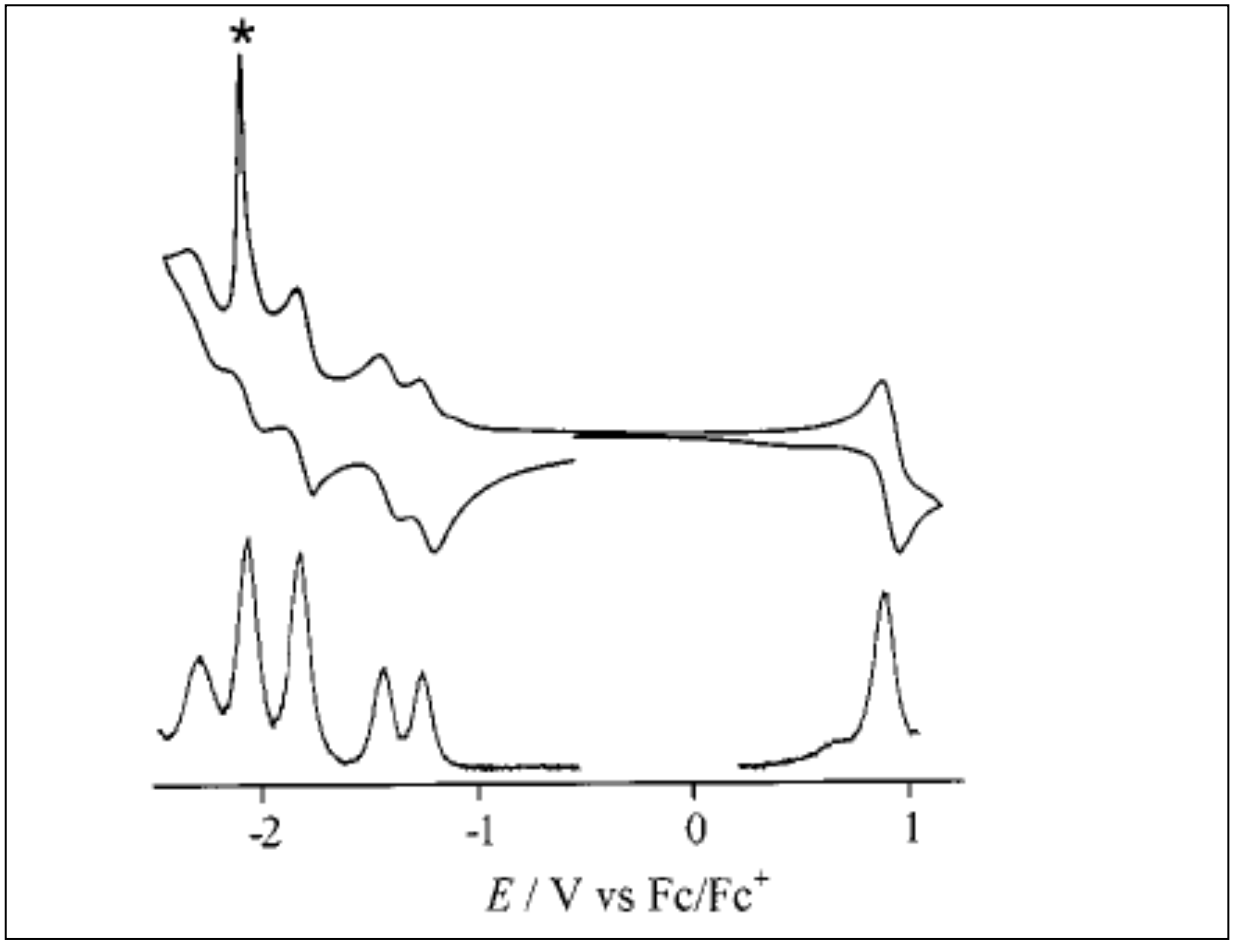

Figure C. 3 Cyclic Voltagram of $\mathbf{1}^{4+}$ in acetonitrile[23]

APPENDIX D

STERN VOLMER PLOT OF $[Ru(bpy)_3]^{2+}$ WITH TEA AND $[B(cat)_2]^{-1}$

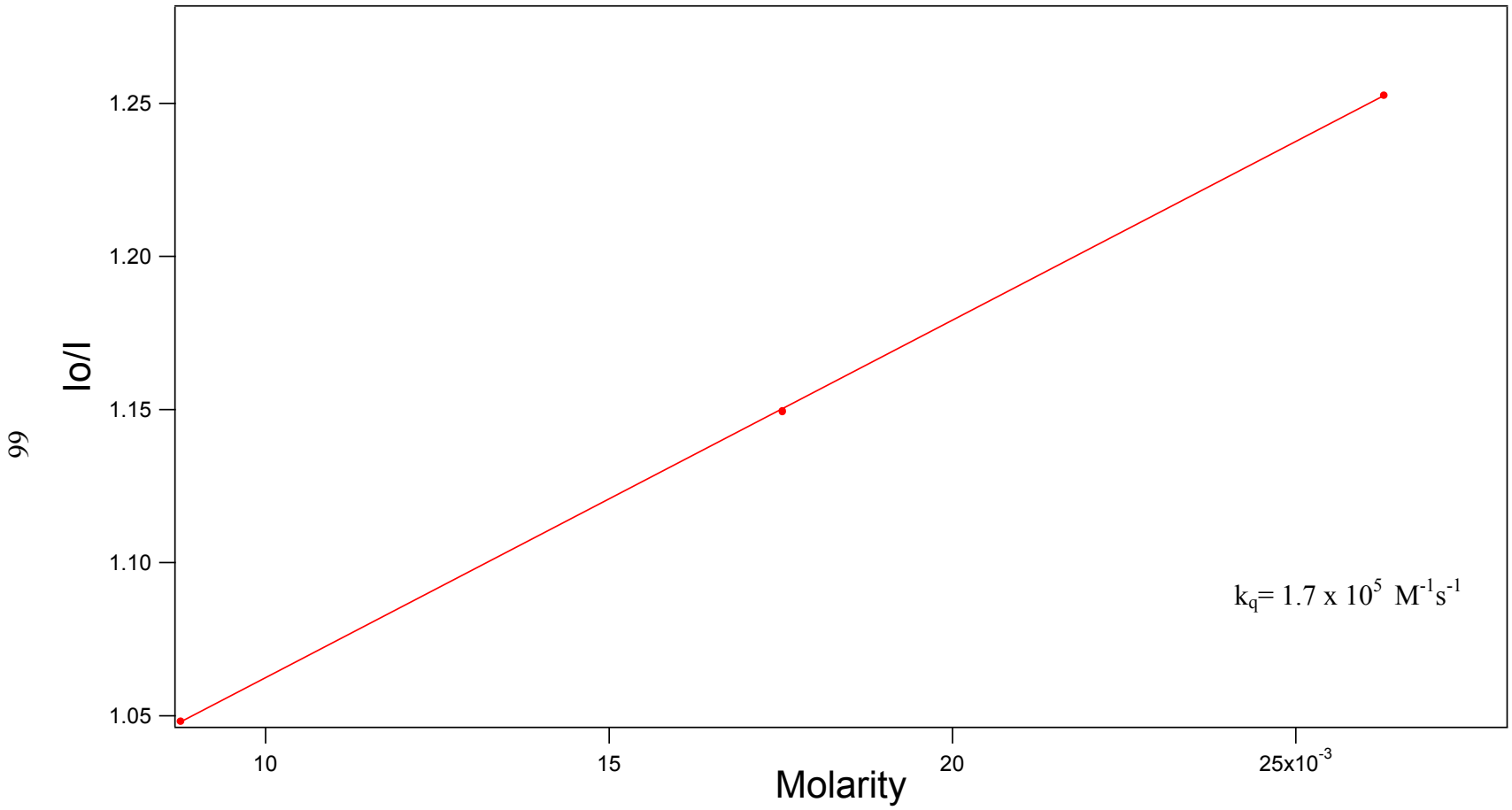

Figure D.1 Plot of 10μM $[Ru(bpy)_3]^{2+}$ and TEOA in **DMF**
Excitation at 451 nm

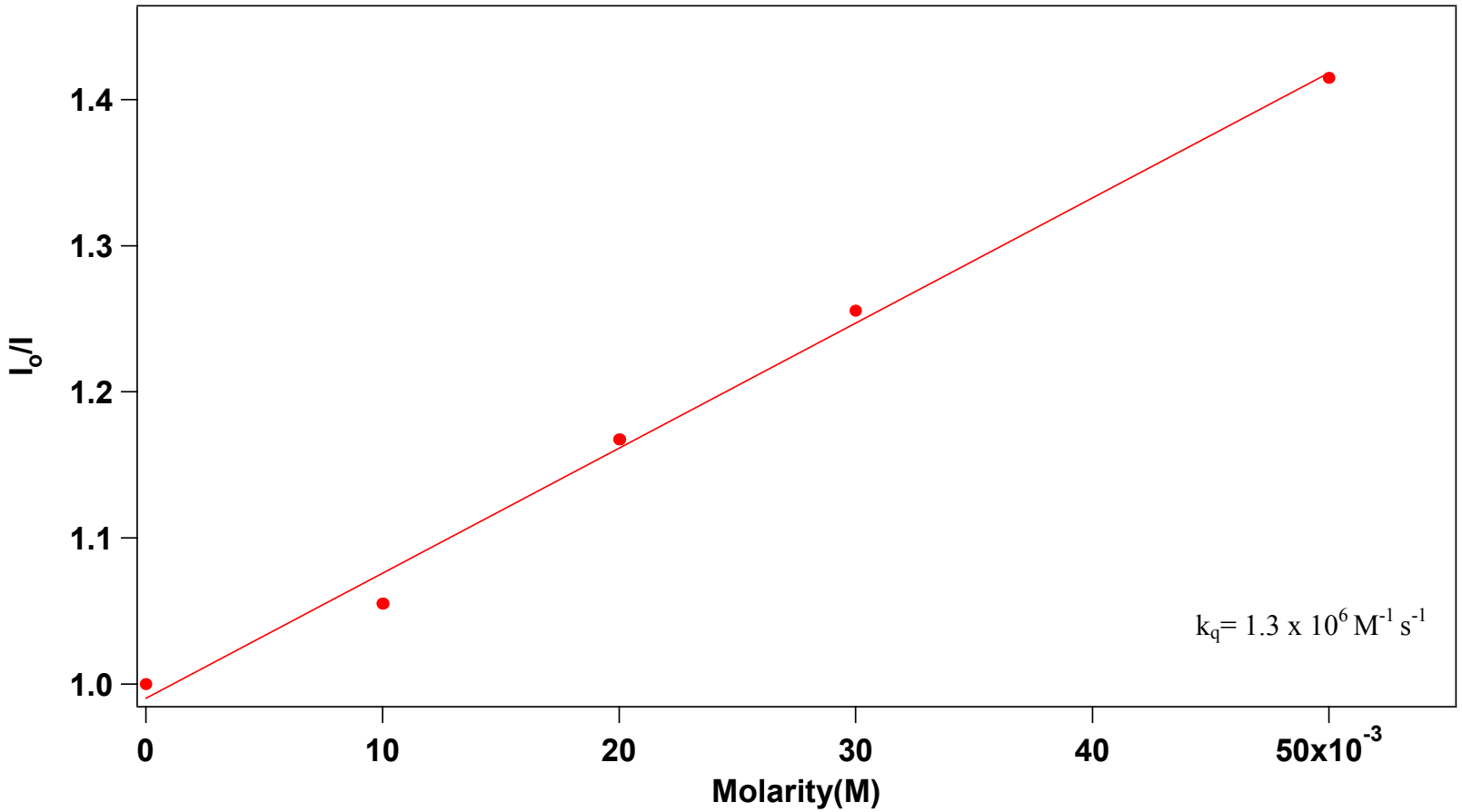

Figure D.2 Plot of 10μM $[Ru(bipy)_3]^{2+}$ and TEA in **MeCN**
Excitation at 451 nm

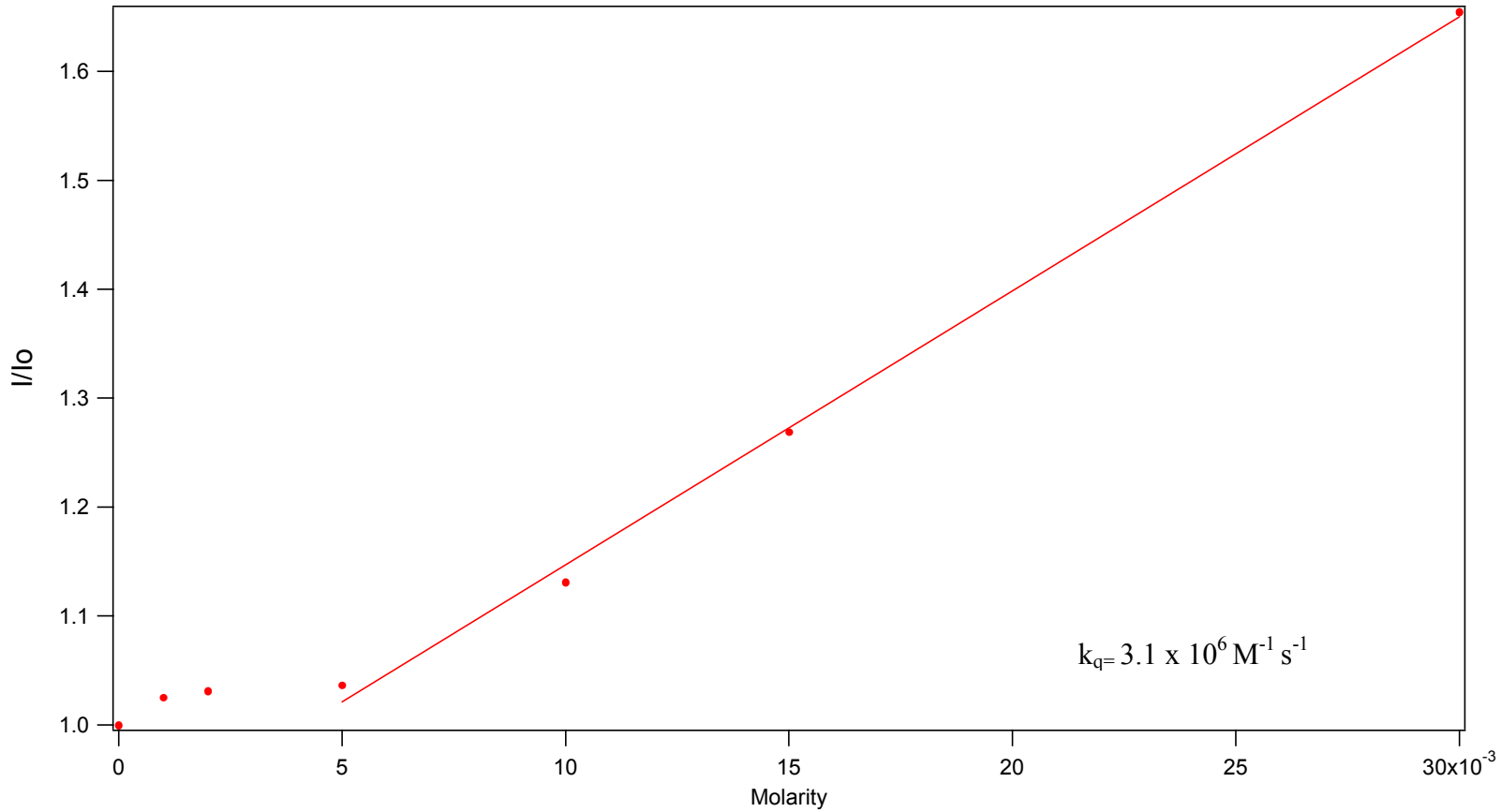

Figure D. 3 Plot of 10 μM $[Ru(bpy)_3]^{2+}$ and $[B(cat)_2]^-$ in 10% water/MeCN mixture
. Excitation at 451 nm

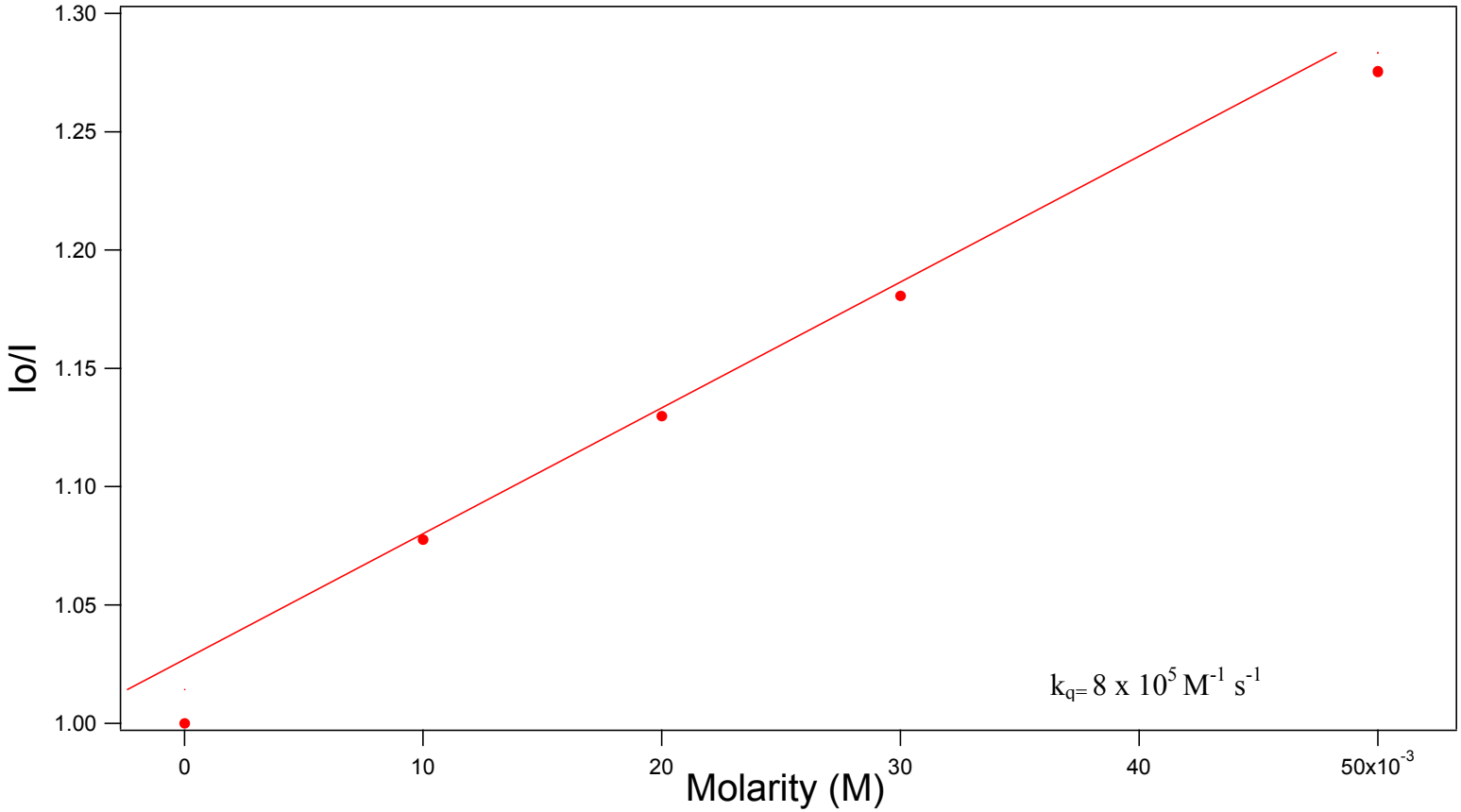

Figure D. 4 Plot of 10 μM $[Ru(bpy)_3]^{2+}$ and TEA in 10% water/MeCN mixture

REFERENCES

1- Kavarnos, G. J.; **1993,** VCH Publishers, Inc. New York

2- Louis, S.; Andreas, Z. *Nature*. , **2001**, 414, 353

3- Gratzel, M. *Nature,* **2001,** 414, 338

4- Villegas, J.M.; Stoyanov, S.R.; Rillema, D.P. *Inorg. Chem.* **2002,** 41, 6688

5- Konduri, R.; Hongwei,Ye.;MacDonnell, F.M.; Serroni, S.; Campagna,S.; Rajeswar, K. *Angew. Chem. Int. Ed*. **2002**, 41, No.17

6- Ellerbrock, J.C.; McLougning, S.M.; Baba, A.I. *Inorg. Chem. Commun.* **2002,** 5, 555

7- Suppan, P. *Chemistry and Light.* The Royal Society of Chemistry, 1994.

8- Roundhill, D. M.; *Photochemistry and Photophysics of Metal Complexes.* Plenum Press, New York, 1994

9- Muray, S. L., Hug, G. L, *Handbook of Photochemsitry.* M. Decker. New York, 1993.

10- Lichtenstein, J.*;* *Materials Performance*, **Oct., 2001**, p.68

11- Ferraoudi, G. J.; **1988.** *John Wiley & Sons, Inc*

12- Barltrop, J. A.; Coyle, J. D. *Principles of Photochemistry.* **1975,** John Wiley & Sons Ltd.

13- Turrro, N.J.; Modern *Molecular Photochemistry.* **1978,** The Benjamin/ Cummings Publishing, Inc

14- Bowen, E.J., *Trans. Faraday Soc.*, 50, 97 (154).

15- Meluish, W.H.; Metcalf, X.S. *J. Chem. Soc.*, 480 (1958).

16- Leite, M.S.S.C.; Razinaqui, K. *Chem. Phys. Lett.*, 4, 35 (1969).

17- Ware, W.R.; Lewis, C. *J. Chem. Phys.*, 57, 3546 (1972).

18- Stern, O.; Volmer, M. *Physik, Z.*, 20, 183 (1919).

19- Calvert, J.G.; Pitts, J.N. *Photochemistry*. John Wiley & Sons, Inc., New York, 1966, pp. 663-70.

20- Neshvad, G.; Hoffman, M.Z. *J. Phys. Chem.* **1989,** 93, 2445-2452

21- Bielski, B. H. *J. Adv. Chem. Ser.* **1982,** 200, 81.

22- Ballardini, R. Varani, G. Indelli, M. T. Scandola, F. Barzani, V.; *J. Am. Chem. Soc.* **1978,** 100, 23, 7219-7223

23- Molnar, M.S.; Nallas, G.; Bridgewater, J. S.; Brewer, K. J. *J. Am. Chem. Soc.* **1994,** 116, 5206-5210

24- Konduri, R.; Hongwei,Ye.;MacDonnell, F.M.; Serroni, S.; Campagna,S.; Rajeswar, K. *Angew. Chem. Int. Ed*. **2002**, 41, No.17

25- Kim, M.J.; Konduri, R.; Ye, H.; MacDonnell, F.M.; Puntoriero, F.; Serroni, S.; Campagna, S.; Holder, T.; Kinsel, G.; Rajeswar, K. *Inorganic Chem.* **2002.** 41, 2471-2476

26- Krich, M.; Lehn, J. M.; Sauvage, J.P.; *Helv. Chimica Acta.,* **1979,** 1345

27- Aterina, C.; Hoffman, M.; *Coordination Chemistry Rewiews*. **1977,** 159, 359-373

28- Alstrum-Acevedo, J. H. Brennaman, M. K. Meyer, T. J.; *Inorganic Chemistry.* **2005,** 44, 6802-6827.

29- Kavarnos, G. J.; Turro, N. J. *Chem. Rev.* **1986**, *86*, 401-449.

30- Adamson A. W.; Fleischauer, P. D.; *Concepts of Inorganic Photochemistry.* **1975.** John Wiley & Sons Ltd.

31- Hoffman, Z. M.; Bolletta, F.; Moggi, L.; Hug, G.; *J. Phys. Chem. Ref. Data,* **1989,** 18, 219-543.

32- Broglia, .F.; Bertolotti, S.G.; Previtali, C. M. ; *J. Photochem. Photophys. A:* Chemistry, **2005**, 170, 261-265

33- Harris, D. A.; *Quantitative Chemical Analysis*. **2003**. W. H Freeman and Company. Ap:24-27

34- Staffilani, M.; Belser, P.; De Cola, L.; Hartl, F.; *Eur. J. Inorg. Chem.* **2002,** 335-339.

35- Finkenstein, M.; Mayeda, E. A.; Ross, S.D.; *J. Org. Chem.* **1975.** 805.

36- Staffilani, M. Belser,P. Hartl, F. Kleverlaan, C.J. De Cola, L.; *J. Phys. Chem. A.* **2002,** 106, 9242-9250.

37- Konduri, R.; Tacconi, N. R.; Rajeswar, K.; MacDonnell, F. M.; *J. Am. Chem. Soc.* **2004.**

38- Wilhelmsson, L. M.; Esbjorner, E. K. ; Westerlund, F.; Norden, B.; Lincoln, P.; *J. Phys. Chem. B,* **2003,** 107, 11784-11793.

39- Yamada, M.; Tanaka, Y.; Yoshimoto, Y.; Kuroda, S.; Shimao, I. *Bull. Chem. Soc. Jpn.* **1992**, *65*, 1006-1011.

40- Hiort, C.; Lincoln, P.; Norde´n, B. *J. Am. Chem. Soc.* **1993**, *115*, 3448-3454

BIOGRAPHICAL INFORMATION

Alper Yarasik was born in Bandirma, Turkey and obtained his B. Sc. at the Koc University, Istanbul, Turkey. He attended the Max-Planck Institute for Chemical Physics of Solids, Dresden, Germany as a research scientist in summer 2000 and 2001. Starting the Fall of 2003, he began attending the University of Texas at Arlington for his Master of Science in chemistry under the supervision of Professor Frederick M. MacDonnell. Alper Yarasik graduated from the University of Texas at Arlington in the Summer of 2006.